bioRxiv preprint doi: https://doi.org/10.1101/2020.12.18.423492; this version posted December 19, 2020. The copyright holder for this preprint (which was not certified by peer review) is the author/funder, who has granted bioRxiv a license to display the preprint in perpetuity. It is made available under aCC-BY-NC-ND 4.0 International license.

TRPM channels mediate learned pathogen avoidance following intestinal distention

Adam Filipowicz and Alejandro Aballay*

Department of Molecular Microbiology & Immunology, Oregon Health & Science University, Portland, OR 97239, USA

*Corresponding author. Email: aballay@ohsu.edu

ABSTRACT

Upon exposure to harmful microorganisms, hosts engage in protective molecular and behavioral immune responses, both of which are ultimately regulated by the nervous system. Using the nematode *Caenorhabditis elegans*, we show that ingestion of *E. faecalis* leads to a fast pathogen avoidance behavior that results in aversive learning. We have identified multiple sensory mechanisms involved in the regulation of avoidance of *E. faecalis,* including the GPCR NPR-1-dependent oxygen-sensing pathway, an ASE neuron-dependent pathway, and an AWB and AWC neuron-dependent pathway. Colonization of the anterior part of the intestine by *E. faecalis* leads to AWB and AWC mediated olfactory aversive learning. Finally, two transient receptor potential melastatin (TRPM) channels, GON-2 and GTL-2, mediate this newly described rapid pathogen avoidance. These results suggest a mechanism by which TRPM channels may sense the intestinal distension caused by bacterial colonization to elicit pathogen avoidance and aversive learning by detecting changes in host physiology.

bioRxiv preprint doi: https://doi.org/10.1101/2020.12.18.423492; this version posted December 19, 2020. The copyright holder for this preprint (which was not certified by peer review) is the author/funder, who has granted bioRxiv a license to display the preprint in perpetuity. It is made available under aCC-BY-NC-ND 4.0 International license.

INTRODUCTION

In order to survive, animals have evolved mechanisms to detect and avoid harmful organisms, including pathogenic bacteria (Kavaliers et al., 2019; Medzhitov et al., 2012). Understanding this complex survival mechanism will ultimately take an interdisciplinary approach. Genetically tractable organisms such as *Caenorhabditis elegans* and *Drosophila melanogaster* have proven to be quite useful in uncovering the molecular and cellular components of pathogen avoidance. In response to pathogen exposure, these relatively simple animals are capable of eliciting avoidance behaviors (Anderson and McMullan, 2018; Cao et al., 2017; Meisel and Kim, 2014; Meisel et al., 2014; Pradel et al., 2007; Reddy et al., 2009; Singh and Aballay, 2019a, 2019b; Soldano et al., 2016; Stensmyr et al., 2012; Styer et al., 2008; Tran et al., 2017; Zhang et al., 2005) along with the activation of well-described microbicidal innate immune pathways (Engelmann et al., 2011; Irazoqui et al., 2010; Singh and Aballay, 2019b; Styer et al., 2008), both of which are regulated by the nervous system (Singh and Aballay, 2020; Wani et al., 2020).

It was recently proposed that bacterial colonization causes a distension of the *C. elegans* intestine that may be used as a general mechanism to activate immune pathways and pathogen avoidance (Kumar et al., 2019; Singh and Aballay, 2019a, 2019b). However, the mechanism by which the nematode senses intestinal distension remains unclear. One possibility is that mechanoreceptors on intestinal cells sense the pressure caused by distention. While no mechanoreceptors have been found to be functional in the *C. elegans* intestine, it does express transient receptor (TRP) channels which, in addition to other roles, could act as mechanoreceptors (Xiao and Xu, 2011). While the TRP vanilloid (TRPV) channel genes *ocr-2* and *osm-9* are known to inhibit avoidance of the pathogen *Pseudomonas aeruginosa* (Singh and Aballay, 2019a), this inhibition is through their role on hyperoxia avoidance rather than direct sensing of bacteria. Moreover, they are not expressed in the *C. elegans* intestine. One TRP channel that is expressed in the *C. elegans* intestine is the thermosensitive channel TRPA-1 (Xiao et al., 2013), TRPA-1 also plays a role in sensory neuron-mediated nose-touch responses (Kindt et al., 2007). Interestingly, the *Drosophila* homolog of this channel was shown to be involved in avoidance of bacterial lipopolysaccharide (LPS), though activity of this channel was localized to gustatory neurons (Soldano et al., 2016). The mammalian digestive system expresses many TRP channels, including members of the TRPA, TRP melastatin (TRPM) and TRPV families, that play a role in processes raging from pain to ion homeostasis (Holzer, 2011). Because nearly all of these channels are conserved across species, identification of their role in pathogen avoidance in *C. elegans* is likely to improve our understanding of pathogen avoidance in a range of organisms.

Here, we present evidence that *C. elegans* avoids *Enterococcus faecalis* faster than *P. aeruginosa.* In contrast to the *P. aeruginosa*-mediated avoidance that requires small RNAs (sRNAs) (Kaletsky et al., 2020), *E. faecalis* does not depend on sRNAs, nor does it require ASI

bioRxiv preprint doi: https://doi.org/10.1101/2020.12.18.423492; this version posted December 19, 2020. The copyright holder for this preprint (which was not certified by peer review) is the author/funder, who has granted bioRxiv a license to display the preprint in perpetuity. It is made available under aCC-BY-NC-ND 4.0 International license.

neurons, full bacterial virulence, or innate immune activation. Instead, avoidance correlates with a rapid expansion of the anterior part of the intestine. This avoidance behavior requires an NPR-1-mediated hyperoxia avoidance process as well as the ASE, AWB, and AWC chemosensory neurons. These latter two neuron pairs regulate an olfactory aversive learning process that underpins avoidance of *E. faecalis.* Finally, we identified two novel regulators of intestinal distention-induced pathogen avoidance: the TRP melastatin (TRPM) channels GON-2 and GTL-2.

RESULTS

E. faecalis elicits fast avoidance in *C. elegans*

C. elegans is a free-living nematode that feeds on organic material rich in microorganisms, and therefore frequently encounters pathogenic bacteria. It has developed behavioral strategies to minimize exposure to these threats. For example, it avoids the pathogenic *P. aeruginosa* bacteria slowly, taking between 12 to 24 hours to execute aerotactic and olfactory aversive learning processes depending on the bacterial growth conditions used (Singh and Aballay, 2019a; Zhang et al., 2005). In contrast, we previously reported that animals quickly avoid the lawns of the Gram-positive pathogens *E. faecalis, E. faecium,* and *S. aureus* (Singh and Aballay, 2019b). Examining this in more detail, we found that animals displayed strong, fast avoidance of monoaxenic lawns of *E. faecalis, E. faecium,* or *S. aureus* grown on brain heart infusion (BHI) media (Figure 1A, 1B, and Figure 1 – figure supplement 1). While population avoidance levels peaked at 4 hours for *E. faecalis*, wild-type animals first leave *E. faecalis* lawns at around 19 minutes on average (Figure 1C). Interestingly, we observed animals frequently exiting and entering the bacterial lawns over time. Quantification of these events revealed a slight imbalance favoring exiting events as early as 1 hour, with this difference growing larger in the 3-4 hour window due to a decrease in the entry events (Figure 1D).

The fast exiting events induced by *E. faecalis* are reminiscent of a *C. elegans* rapid aversive behavior elicited by exposure to a dry-drop of dodecanoic acid, a toxin secreted by *Streptomyces* (Tran et al., 2017). However, implementing this dry-drop assay with *E. faecalis* or *E. faecium* did not induce an aversive response (Figure 1 – figure supplement 1), indicating that direct contact with live replicating bacteria is required for the rapid avoidance of *E. faecalis* or *E. faecium*. Rapid aversion alone also cannot explain the re-entry events. Instead, it is likely that there is a balance of attraction and aversion to *E. faecalis* that changes over the course of exposure. Thus, the animals learn to avoid *E. faecalis* quickly after exposure. This process likely involves sensory pathways, as animals with loss-of-function mutations in *tax-2,* a subunit of a cGMP-gated-ion-channel important for sensory neuron function (Coburn and Bargmann, 1996), show slowed avoidance (Figure 1C). Because it has recently been suggested that the sensation of a bacterial sRNAs is at least partly responsible for learned *P. aeruginosa* avoidance (Kaletsky et al., 2020), we examined whether RNA from *E. faecalis* may also elicit avoidance. Unlike RNA

bioRxiv preprint doi: https://doi.org/10.1101/2020.12.18.423492; this version posted December 19, 2020. The copyright holder for this preprint (which was not certified by peer review) is the author/funder, who has granted bioRxiv a license to display the preprint in perpetuity. It is made available under aCC-BY-NC-ND 4.0 International license.

from *P. aeruginosa*, RNA from *E. faecalis* fails to induce avoidance (Figure 1E). The fact that exposure to bacterial sRNAs only accounts for ~25% of the avoidance of *P. aeruginosa,* and that they have no role in avoidance of *E. faecalis,* suggests that another pathway is required to induce pathogen avoidance.

Anterior intestinal distention elicits avoidance of *E. faecalis* independently of virulence

Two other potential pathways for induction of avoidance are sensation of intestinal distention or bacterial metabolites. The bacterial metabolite serrawettin W2 is responsible for the avoidance of *S. marcescens* (Pradel et al., 2007). Even though secondary metabolites phenazine-1-carboxamide and pyochelin produced by *P. aeruginosa* are insufficient for the elicitation of pathogen avoidance (Singh and Aballay, 2019a), they are sensed by *C. elegans* as they elicit induction of DAF-7/TGF-β in ASJ neurons (Meisel et al., 2014). However, *E. faecalis* does not increase expression of DAF-7 in the ASJ neurons (Meisel et al., 2014), further strengthening the idea that direct contact with this pathogen rather than metabolite sensing induces avoidance.

To determine whether intestinal distention plays a role in avoidance of *E. faecalis*, we measured the diameter of the intestinal lumen of animals fed either *E. coli, P. aeruginosa,* or *E. faecalis* grown on BHI. There was significant expansion of the anterior part of the intestine of animals feeding on *E. faecalis* compared to *E. coli* even at 1 hour, with distention persisting at 4 hours (Figure 2A and B). The medial part of the intestine was not significantly bloated at 1 hour compared to animals fed *E. coli*, but was bloated at 2 and 4 hours. The anterior part of the intestine was slightly bloated in animals feeding on *P. aeruginosa* compared to *E. coli* at 4 hours, but was otherwise not bloated. Both parts of the intestine, but especially the anterior portion, were filled with live *E. faecalis*, as determined through the use of an *E. faecalis* strain expressing GFP, while the intestine of animals fed *E. coli* or *P. aeruginosa* expressing GFP were relatively empty and not distended (Figure 2C). It is therefore likely that fast accumulation of *E. faecalis* in the anterior intestine induces an aversive response to the pathogen, leading to avoidance. RNA interference (RNAi)-mediated knockdown of *nol-6*, a nucleolar RNA-associated protein, reduces colonization and distention of the intestine by microbial pathogens (Fuhrman et al., 2009). Furthermore, knockdown of *nol-6* delays avoidance of *P. aeruginosa* by delaying intestinal distention (Singh and Aballay, 2019a; Figure 2 - figure supplement 1). Therefore, we tested both *nol-6* RNAi and a *nol-6* loss-of-function (lf) mutant (*nol-6(ac1)*) for avoidance of *E. faecalis.* Avoidance for both the mutant and *nol-6* RNAi remained at wild-type levels (Figure 2D). Interestingly, while anterior intestinal distension was observed in both *nol-6(ac1)* and *nol-6* RNAi animals fed *E. faecalis* at 4 hours, the middle part of the intestine did not display significant distention (Figure 2E, F, and Figure 2 – figure supplement 1). This suggests that the anterior, but not medial, intestinal distention triggers avoidance of *E. faecalis*.

bioRxiv preprint doi: https://doi.org/10.1101/2020.12.18.423492; this version posted December 19, 2020. The copyright holder for this preprint (which was not certified by peer review) is the author/funder, who has granted bioRxiv a license to display the preprint in perpetuity. It is made available under aCC-BY-NC-ND 4.0 International license.

To determine whether bacterial virulence is required for anterior intestine distention induced avoidance of *E. faecalis*, we used a strain of *E. faecalis* lacking the *fsrB* gene (*E. faecalis ΔfsrB*), a gene important for quorum sensing, which displays significantly reduced virulence across multiple animal models (Garsin et al., 2001; Mylonakis et al., 2002; Sifri et al., 2002). Surprisingly, this avirulent strain also elicits avoidance (Figure 3A). Lending further evidence to the notion that virulence plays no role in avoidance, *E. faecium*, a related enterococcal species that is non-pathogenic to *C. elegans* (Garsin et al., 2001; Yuen and Ausubel, 2018), also elicits avoidance (Figure 1B). While *E. faecium* is non-pathogenic to *C. elegans* it does cause an innate immune response (Yuen and Ausubel, 2018), raising the possibility that an early immune response may be responsible for alerting the animal to avoid *E. faecalis* and related species upon ingestion.

Therefore, we examined the *in vivo* expression of two immune pathway markers, *clec-60* (Irazoqui et al., 2010; Yuen and Ausubel, 2018) and *ilys-3* (Gravato-Nobre et al., 2016; Irazoqui et al., 2010; Yuen and Ausubel, 2018), to determine whether an immune response was mounted at these early timepoints. While a later immune response could be observed, there was no evidence of an immune response at timepoints where early avoidance of *E. faecalis* is observed (Figure 3B-D). As shown in Figure 3E, *E. faecalis ΔfsrB* induces anterior intestinal distension. Altogether, these results suggest that virulence and immune pathway activation is not necessary for anterior distension and avoidance of *E. faecalis*, differentiating this avoidance mechanism further from that induced by *P. aeruginosa*, which requires virulence and intestine-wide distension (Kumar et al., 2019; Singh and Aballay, 2019a, 2019b).

NPR-1 and TAX-2/4 pathways regulate avoidance of *E. faecalis* and *P. aeruginosa*

NPR-1, known to play a role in *C. elegans* survival and behavior on pathogens (Meisel and Kim, 2014; Reddy et al., 2009; Styer et al., 2008), is responsible for the intestinal distention induced avoidance behavior on *P. aeruginosa*. We hypothesized that NPR-1 would also play a role in avoidance of *E. faecalis.* As a first step to test this, we measured avoidance of *E. faecalis* in two *npr-1 (lf)* mutants and found that both displayed decreased avoidance compared to wild-type animals (Figure 4A).

Inhibition of NPR-1 elicits avoidance of high oxygen (de Bono and Bargmann, 1998; Chang et al., 2006; Rogers et al., 2003), resulting in suppression of *P. aeruginosa* avoidance (Reddy et al., 2009; Styer et al., 2008), as the bacterial lawns have low oxygen due to microbial metabolism (Reddy et al., 2011). To test whether that is the case with avoidance of *E. faecalis,* wild-type and *npr-1 (lf)* animals were placed into hypoxia (8% oxygen) chambers and scored for avoidance. In this low oxygen environment, both *npr-1(ad609)* and *npr-1(ok1447)* displayed wild-type levels of avoidance (Figure 4B). Furthermore, when animals were taken out of the low oxygen environment and allowed to roam at atmospheric oxygen levels for one-hour, wild-type

bioRxiv preprint doi: https://doi.org/10.1101/2020.12.18.423492; this version posted December 19, 2020. The copyright holder for this preprint (which was not certified by peer review) is the author/funder, who has granted bioRxiv a license to display the preprint in perpetuity. It is made available under aCC-BY-NC-ND 4.0 International license.

animals remained off the *E. faecalis* lawns while both *npr-1(lf)* strains migrated back onto the lawns (Figure 4C), indicating that hyperoxia avoidance overrides pathogen avoidance in *npr-1(lf)* animals.

Hyperoxia avoidance in *npr-1(lf)* animals requires the transient receptor potential channel vanilloid (TRPV) genes *ocr-2* and *osm-9* (de Bono et al., 2002; Chang et al., 2006; Singh and Aballay, 2019a). Loss-of-function mutations in these genes results in decreased hyperoxia avoidance, and should thus lead to increased pathogen avoidance. Indeed, while loss-of-function mutants in both genes displayed avoidance levels similar to wild-type animals at 4 hours (Figure 4 – supplement 1), their rate of avoidance was faster than that of wild-type animals (Figure 4 – supplement 1). Hyperoxia avoidance of *npr-1(lf)* nematodes also depends on functional *gcy-35, tax-2,* and *tax-4* genes (Chang et al., 2006; Gray et al., 2004). GCY-35 is a soluble guanylyl cyclase (sGC) that binds directly to molecular oxygen (Cheung et al., 2004) while TAX-2 and TAX-4 are two subunits of a cGMP-gated-ion-channel (Coburn and Bargmann, 1996) thought to act downstream of GCY-35 (Coates and de Bono, 2002; Gray et al., 2004). Through the activity of GCY-35 and TAX-2/TAX-4, the sensory neurons AQR, PQR, and URX drive avoidance of high oxygen. We tested double loss-of-function mutants of *gcy-35*, *tax-2,* or *tax-4* and *npr-1*, hypothesizing that *gcy-35*, *tax-2*, and *tax-4* mutations would suppress the lack of pathogen avoidance of *npr-1(ad609)* animals. While this was indeed the case for *gcy-35* mutation, *tax-2* and *tax-4* mutations failed to suppress the lack of avoidance of *E. faecalis* exhibited by *npr-1(ad609)* animals (Figure 4D). These results suggest that TAX-2 and TAX-4 function in neurons other than NPR-1-expresing cells to mediate pathogen avoidance.

We next tested the role of TAX-2 and TAX-4 in the NPR-1-mediated avoidance of *P. aeruginosa* using double mutants for *tax-2* or *tax-4* and *npr-1*. Surprisingly, and in contrast to avoidance of *E. faecalis*, *tax-2* but not *tax-4* mutation suppressed the avoidance of *P. aeruginosa* of *npr-1(ad609)* animals (Figure 4D). The discrepancy between the double mutants is that the *tax-2(p694)* allele used only affects a subset of the *tax-2* expressing neurons (Harris et al., 2014). The *tax-4(p678)* allele, in contrast, affects all *tax-4*-expressing neurons (Figure 4E). Thus, the neurons affected by the *tax-4(p678)* allele, but spared by the *tax-2(p694)* allele, most likely play a role in avoidance of *P. aeruginosa* independent from the NPR-1 pathway. The results from the *E. faecalis* experiments, on the other hand, suggest that the *tax-2(p694)* allele covers additional neurons that regulate avoidance of that bacteria. To confirm this, we used single loss-of-function mutants for *tax-2* and *tax-4*, including a strain carrying an allele that affects expression in all *tax-2* expressing neurons (*tax-2(p671)*). We indeed found that all strains tested displayed decreased avoidance of *E. faecalis* compared to wild-type animals, while only *tax-2(p671)* and *tax-4(p678)* mutants displayed decreased avoidance of *P. aeruginosa* (Figure 4F).

ASE, AWB, and AWC neurons mediate avoidance of *E. faecalis*

bioRxiv preprint doi: https://doi.org/10.1101/2020.12.18.423492; this version posted December 19, 2020. The copyright holder for this preprint (which was not certified by peer review) is the author/funder, who has granted bioRxiv a license to display the preprint in perpetuity. It is made available under aCC-BY-NC-ND 4.0 International license.

We turned our attention to uncovering the specific neurons in the TAX-2/TAX-4-dependent pathway that regulate avoidance of both *E. faecalis* and *P. aeruginosa*. To identify the neuron(s) responsible for *E. faecalis* avoidance, we employed two strategies. First, we asked whether *tax-2* expression in individual neurons would rescue the lack of pathogen avoidance of *tax-2(p694)* animals. This revealed that *tax-2* expression in ASE neurons was sufficient for pathogen avoidance, while *tax-2* expression in the AQR, PQR, and URX neurons, had no effect (Figure 5A). Second, we used animals lacking ASE neurons and the individual AWB, AWC, and ASI neurons, which are spared by the *tax-2(p694)* allele. The results confirmed the involvement of ASE neurons in *E. faecalis* avoidance and showed that AWB and AWC neurons are also necessary (Figure 5B).

For avoidance of *P. aeruginosa,* we also employed the genetic ablation strategy, which revealed the requirement of AWB and AWC neurons (Figure 5B). Confirming the results of the *tax-2* experiments, ASE neurons were not required for avoidance of *P. aeruginosa*. We also confirmed a previous report that ASI neurons, but not ASH neurons, are required for avoidance of *P. aeruginosa* (Cao et al., 2017), while showing that neither is required for avoidance of *E. faecalis* (Figure 5B). Using a two-choice assay where, unlike the pathogen avoidance assay that only uses *P. aeruginosa*, animals are given a choice between *E. coli* and *P. aeruginosa*, it was shown that ASI neurons respond to *P. aeruginosa* RNAs by eliciting avoidance (Kaletsky et al., 2020). Using both avoidance and choice assays, we found that animals lacking ASI neurons fail to avoid *P. aeruginosa* after total RNA exposure (Figure 5C, D). These results are consistent with the idea that ASI neurons are capable of sensing *P. aeruginosa* RNAs and that *E. faecalis* RNAs do not induce avoidance (Figure 1E). Altogether, these results suggest that regulation of behavioral immunity is pathogen-specific (Figure 5E).

AWB and AWC neurons are necessary for aversive olfactory learning following ingestion of *E. faecalis*

Our data suggested that avoidance of *E. faecalis* represented an aversive learning process (Figure 1D), but we tested this directly. AWB and AWC neurons are known to play a role in odor preference and olfactory aversive learning in *C. elegans* in the context of *P. aeruginosa* (Ha et al., 2010; Harris et al., 2014). Because AWB and AWC neurons are also involved in avoidance of *E. faecalis*, we hypothesized that odor preference and olfactory aversive learning may also play a role in avoidance of *E. faecalis*. We first set out to establish the naïve preference of *C. elegans* when given the choice between *E. coli* and *E. faecalis.* We used a two-choice assay in which animals were able to roam for one hour on test plates containing *E. coli* and *E. faecalis* lawns on opposite sides of the plates before scoring animals based on lawn occupancy. Under this condition, animals showed a preference for *E. coli* over *E. faecalis*; however, if animals were instead paralyzed upon approaching the lawns, they displayed a preference for *E. faecalis* (Figure 6A). We hypothesized that there is an initial attraction to *E. faecalis* that is quickly

bioRxiv preprint doi: https://doi.org/10.1101/2020.12.18.423492; this version posted December 19, 2020. The copyright holder for this preprint (which was not certified by peer review) is the author/funder, who has granted bioRxiv a license to display the preprint in perpetuity. It is made available under aCC-BY-NC-ND 4.0 International license.

overcome after feeding on it, such that animals go towards the familiar *E. coli* lawn instead. Paralyzing animals on lawn arrival captures the initial choice, while allowing them to freely roam captures the aversive learning behavior. We further hypothesized that this attraction-aversion dynamic was at least partly olfactory, based on neuron ablation results (Figure 5), and evidence that *tax-2(lf)* leads to significantly delayed lawn exiting (Figure 1C).

To directly test the idea of an initial odor attraction, we modified the choice assay by attaching plugs of agar with bacterial lawns on opposite sides of the lids of empty test plates (Figure 6B, schematic), preventing the animals to get in direct contact with the bacteria. We then placed the anesthetic sodium azide on the test plate surface underneath the bacteria plugs and placed animals on the center of the plate, allowing them to migrate towards one side or the other. This revealed a naïve preference for the odor of *E. faecalis* over *E. coli* (Figure 6B, left). Both *tax-2(p671)* and *tax-4(p678)* mutants displayed decreased naïve odor preferences but *tax-2(p694)* did not. This result is consistent with the idea that the *tax-2* and *tax-4* expressing neurons AWB and AWC are responsible for establishing the naïve odor preference. Indeed, ablating them also resulted in a decreased preference (Figure 6B, left). We next asked whether trained animals that were allowed to ingest *E. faecalis* would switch their odor preference. The animals were trained by exposing them to *E. faecalis* for four hours using the same plate setup that had been used for the avoidance assays. Then, the trained animals were transferred to the lid-choice testing plates. A marked shift in preference was observed for trained wild-type animals that was not seen in *tax-2(p671)*, *tax-4(p678),* or AWB and AWC ablated strains (Figure 6B, left). The *tax-2(p694)* mutants, on the other hand, behaved like wild-type animals. The learning index for each strain also highlights that aversive olfactory learning takes place in wild-type and *tax-2(p694)* animals but not in *tax-2(p671)* or *tax-4(p678)* mutants or AWB and AWC ablated strains (Figure 6B, right). Thus, the *tax-2* and *tax-4* expressing AWB and AWC neurons are necessary both for establishing a naïve preference and for aversive olfactory learning following ingestion of *E. faecalis* over a period of four hours.

The TRPM channels *gon-2* and *gtl-2* are required for distention-induced pathogen avoidance

It remains unclear how *C. elegans* senses intestinal bloating in order to execute pathogen avoidance, either for *P. aeruginosa* or *E. faecalis.* Because TRP channels could be mechanoreceptors (Xiao and Xu, 2011) capable of sensing the intestinal distension caused by microbial colonization, we screened animals with loss-of-function mutations in 5 TRP-encoding genes for avoidance of *E. faecalis* and found that two members of the TRPM subfamily, *gon-2* and *gtl-2,* negatively affected avoidance of *E. faecalis* (Figure 7 – supplement 1). GON-2 is expressed mainly in the gonad and intestine while GTL-2 is expressed primarily in the excretory system, hypodermis, and pharynx (Teramoto et al., 2005). Because *gon-2* mutants are known to have abnormal gonad development, and the germline has previously been shown to be involved in pathogen avoidance and immunity (Kaletsky et al., 2020; Moore et al., 2019;

bioRxiv preprint doi: https://doi.org/10.1101/2020.12.18.423492; this version posted December 19, 2020. The copyright holder for this preprint (which was not certified by peer review) is the author/funder, who has granted bioRxiv a license to display the preprint in perpetuity. It is made available under aCC-BY-NC-ND 4.0 International license.

TeKippe and Aballay, 2010), we tested whether the effect of *gon-2(lf)* mutations on pathogen avoidance was due to perturbed gonad development. We took advantage of the fact that the Gon phenotype is temperature sensitive (high penetrance at 25°C and low penetrance at 15°C) and compared avoidance results for both *E. faecalis* and *P. aeruginosa* at both temperatures. For *P. aeruginosa*, *gon-2(lf)* animals raised at 25°C failed to avoid, while animals raised at 15°C avoided like wild-type animals (Figure 7A and B). For *E. faecalis*, *gon-2(lf)* animals failed to avoid at both temperatures (Figure 7A and B), suggesting that the germline does not play a role in the control of avoidance of this pathogen. Furthermore, *glp-1(e2141)* mutants, which lack most germline cells due to defects in mitotic and meiotic division (Austin and Kimble, 1987; Crittenden et al., 1994), behave similarly to *gon-2(lf)* mutant animals on both pathogens (Figure 7A and B). This suggests that *gon-2(lf)* animals fail to avoid *P. aeruginosa* specifically because of a lack of gonad development, while for *E. faecalis* the effect on avoidance is independent of the germline. Unlike *gon-2(lf)*, *gtl-2(n2618)* animals failed to avoid *E. faecalis* but not *P. aeruginosa* (Figure 7A and B).

We hypothesized that the effect observed for *gon-2(lf)* and *gtl-2(n2618)* animals was due to an inability to sense intestinal distention either directly or indirectly. It was previously shown that knockdown of *aex-5* leads to defects in the defecation motor program and subsequent intestinal distention by the accumulation of bacteria, resulting in increased avoidance of even non-pathogenic *E. coli* (Singh and Aballay, 2019a). Interestingly, *gon-2(lf)* mutants failed to exhibit such avoidance on *E. coli* HT115 after knockdown of *aex*-5, while *gtl-2(n2618)* mutants behaved like wild-type animals (Figure 7C). These results are consistent with the different types of distention caused by *E. faecalis* and *P. aeruginosa*, with the former causing a more severe but localized distention of the anterior intestine and the latter causing a distention along the entire length of the intestine, which seems to require the germline to elicit avoidance. As shown in Figure 7D, both *gon-2* and *gtl-2* mutants suppressed the *aex*-5 knockdown avoidance phenotype on *E. faecalis*, suggesting that both TRPM channels are necessary for sensing the anterior intestinal distention caused by *E. faecalis.*

DISCUSSION

This study establishes that *E. faecalis* infection in *C. elegans* leads to anterior intestinal distention which results in a rapid pathogen avoidance behavior, regulated by NPR-1-mediated hyperoxia avoidance, TAX-2/4 expressing AWB, AWC, and ASE sensory neurons, and the TRPM channels GON-2 and GTL-2. In contrast, avoidance of *P. aeruginosa* uses different mechanisms that involve intestine-wide distention, germline mediated-signaling, and sensing of bacterial sRNAs via an ASI neuronal pathway (Figure 7E). Thus, bacterial context is important for the elicitation of pathogen avoidance behaviors. This context-dependence makes it likely that using *C. elegans* may lead to the discovery of new components of sensory pathways involved in pathogen avoidance and help to elucidate how physiological information from the site of

bioRxiv preprint doi: https://doi.org/10.1101/2020.12.18.423492; this version posted December 19, 2020. The copyright holder for this preprint (which was not certified by peer review) is the author/funder, who has granted bioRxiv a license to display the preprint in perpetuity. It is made available under aCC-BY-NC-ND 4.0 International license.

infection is relayed to the nervous system. This was indeed highlighted by the identification of ASE neurons and GTL-2 as being necessary for avoidance of *E. faecalis* but not *P. aeruginosa,* and the requirement of the germline in avoidance of *P. aeruginosa* but not *E. faecalis.*

The decision to leave a bacterial lawn represents a dynamic balance between risk and reward for *C. elegans*, with feeding and food choice being critical for survival and propagation (Kiyama et al., 2012; Milward et al., 2011; Shtonda and Avery, 2006). Initially, the balance may be towards staying on the lawn, as it could be an area of high reward in the form of food. However, depending on the quality of the food, its availability, and its potential noxious qualities, the balance may swing towards bacterial avoidance, as the lawn becomes either an area of low reward (depleted or low-quality) or an area of high risk (pathogenic). The frequent entering and exiting events of animals on lawns of *E. faecalis* (Figure 1C and 1D) may be indicative of this dynamic balance. Multiple sensory inputs or physiological states such as oxygen level, odors, tastes, mechanosensation, pain, and hunger must be integrated in order to evaluate the environment and come to a decision. These cues are most likely integrated in the interneurons of *C. elegans,* which are downstream of the sensory neurons (Metaxakis et al., 2018; Summers et al., 2015; Wilson et al., 2017).

The involvement of ASE neurons, largely described as gustatory neurons, in the avoidance of *E. faecalis* (Figures 3A and B) suggests that taste may play a role in pathogen avoidance in *C. elegans* in certain contexts. ASE neurons have also been shown to be CO2 sensors (Bretscher et al., 2011), and polymodal sensory neurons are common in *C. elegans* (Kaplan and Horvitz, 1993; Metaxakis et al., 2018), raising the possibility that ASE sensation of carbon dioxide, and not gustation, may elicit avoidance of *E. faecalis*. Additionally, a recent study implicated ASEL as a secondary sensory neuron in the detection of the food odor benzaldehyde (Leinwand et al., 2015). Interestingly, AWC neurons are also recruited into a salt-sensing circuit via neuropeptide signaling from ASE neurons depending on salt concentration changes (Leinwand and Chalasani, 2013), leaving open the possibility that AWC neurons also play a role in avoidance of *E. faecalis* (Figures 3A and B) not only through olfactory aversive learning (Figure 6C) but through taste aversive learning. Further studies will need to be conducted to determine which possible sensory modality is important for ASE-dependent and AWC-dependent avoidance of *E. faecalis*. ASE neurons were also identified as part of the complex circuitry underlying the decision to leave a resource-depleted food patch, possibly via carbon dioxide sensing (Milward et al., 2011), suggesting an interesting link between pathogen avoidance and adaptive food leaving.

AWB and AWC involvement in odor preference and olfactory aversive learning is well-established in various contexts (Ha et al., 2010; Harris et al., 2014; Yoshida et al., 2012), and the present study extends this to *C. elegans* interactions with *E. faecalis* (Figure 6C) while providing direct evidence of their involvement in avoidance for both *E. faecalis* and *P. aeruginosa* (Figures

bioRxiv preprint doi: https://doi.org/10.1101/2020.12.18.423492; this version posted December 19, 2020. The copyright holder for this preprint (which was not certified by peer review) is the author/funder, who has granted bioRxiv a license to display the preprint in perpetuity. It is made available under aCC-BY-NC-ND 4.0 International license.

3A and B). The olfactory circuitry in *C. elegans* has been described in detail (Chalasani et al., 2007; Leinwand et al., 2015). AWC neurons also communicate and receive feedback from other interneurons through the use of neuropeptides, such as the NLP-1-NPR-11-INS-1 feedback loop between AWC and AIA interneurons (Chalasani et al., 2010). The circuitry for olfactory aversive learning has also received extensive study in the context of *P. aeruginosa* with serotonin and various neuropeptides playing crucial roles in learning and foraging states (Chen et al., 2013; Fadda et al., 2020; Flavell et al., 2013; Ha et al., 2010; Harris et al., 2014; Zhang et al., 2005). Interestingly, both AWB and AWC neurons were previously shown to play a role in avoidance of normally attractive food following undernourishment (Olofsson, 2014), providing another link between pathogen avoidance behavior and foraging. Furthermore, in a recent study, the transcription factor Nrf2/*skn-1* was shown to be required in the AIY interneuron for the integration of information from ASE and AWC neurons during foraging (Wilson et al., 2017). Whether this same AIY neuronal integration is required for pathogen avoidance remains to be seen. Previous work in *Drosophila* has also revealed olfactory-mediated avoidance of harmful microbes (Stensmyr et al., 2012), illustrating that similar mechanisms are at play across different species.

The discovery of *gon-2* and *gtl-2* playing a role in pathogen avoidance is novel. The most well-known impact of loss of *gon-2* function is severe impairment of gonadogenesis due to disruption of gonadal cell divisions (Sun and Lambie, 1997). This impairment is most likely responsible for the results observed for avoidance of *P. aeruginosa* (Figure 7A and B), as the germline and associated tissues are necessary for this avoidance behavior (Kaletsky et al., 2020; Moore et al., 2019; TeKippe and Aballay, 2010). The results of the *glp-1* experiments (Figure 7A and B) further support this idea. However, the germline seems to play no role in avoidance of *E. faecalis,* and therefore other functions of *gon-2* and *gtl-2* may be responsible. The germline plays a role in a transgenerational learned avoidance of *P. aeruginosa* (Moore et al., 2019), but the lack of involvement of the germline (Figure 7A and B), bacterial sRNAs (Figure 3C), and ASI neurons (Figure 3B) in avoidance of *E. faecalis* suggest that such a process may not exist in the case of *E. faecalis* infection. Because *gon-2* is known to be highly expressed in the intestine, where it is responsible for electrolyte homeostasis (Teramoto et al., 2005), it may function as an intestinal receptor for the changes elicited by *E. faecalis* colonization. Magnesium excretion, and perhaps additional electrolytes, requires the activity of *gtl-2* in the excretory cell (Teramoto et al., 2010). Thus, it is possible that the role of *gon-2* and *gtl-2* in pathogen avoidance is related to sensation of an electrolyte perturbance caused by intestinal distention. These TRPM channels could also be mechano-nociceptors, as described in other animal models (Mueller-Tribbensee et al., 2015), that sense intestinal distention directly. Because the intestine is not directly innervated, any signal coming from it must be extra-synaptic, such as an intestinal neuropeptide (Lee and Mylonakis, 2017). All animals are under pressure to develop behaviors

bioRxiv preprint doi: https://doi.org/10.1101/2020.12.18.423492; this version posted December 19, 2020. The copyright holder for this preprint (which was not certified by peer review) is the author/funder, who has granted bioRxiv a license to display the preprint in perpetuity. It is made available under aCC-BY-NC-ND 4.0 International license.

that allow them to flee potential pathogens (Sarabian et al., 2018). Future work will continue to elucidate the mechanisms underlying avoidance of pathogenic threats.

MATERIALS AND METHODS

Bacterial strains

The following bacterial strains were used: *Enterococcus faecalis* OG1RF, *E. faecalis* OG1RF Δ*fsrB*, *E. faecalis* OG1RF-GFP, *E. faecium* E007, *Escherichia coli* OP50, *E. coli* OP50-GFP, *E. coli* HT115(DE3), *Pseudomonas aeruginosa* PA14, *P. aeruginosa* PA14-GFP, and *Staphylococcus aureus* NCTC8325. *E. coli* and *P. aeruginosa* bacterial strains were grown in Luria-Bertani (LB) broth at 37°C while the rest were grown in brain-heart infusion (BHI) broth at 37°C. All sources are listed in the Key Resources table.

C. elegans strains and growth conditions

C. elegans hermaphrodites were maintained on *E. coli* at 20°C unless otherwise indicated. Bristol N2 was used as the wild-type control unless otherwise indicated. All other strains and their sources are listed in the Key Resources table.

RNA interference (RNAi)

RNAi was used to generate loss-of-function RNAi phenotypes by feeding nematodes *E. coli* strain HT115(DE3) expressing double-stranded RNA (dsRNA) homologous to a target gene (Fraser et al., 2000; Timmons and Fire, 1998). RNAi was carried out as described previously (Singh and Aballay, 2017). Briefly, *E. coli* with the appropriate vectors were grown in LB broth containing ampicillin (100 µg/mL) and tetracycline (12.5µg/mL) at 37°C overnight and plated onto NGM plates containing 100 µg/mL ampicillin and 3 mM isopropyl β-D-thiogalactoside (IPTG) (RNAi plates). RNAi-expressing bacteria were allowed to grow for two days at 20°C. Gravid adults were transferred to RNAi-expressing bacterial lawns and allowed to lay eggs for 5 hr. The gravid adults were removed, and the eggs were allowed to develop at 20°C to young adults for subsequent assays. The RNAi clones were from the Ahringer RNAi library.

Lawn avoidance assays

Bacterial cultures were grown by inoculating individual bacterial colonies into 2 mL of either LB or BHI broth and growing them for 5-6 hr on a shaker at 37°C. Then, 20-µL of the culture was plated onto the center of 3.5-cm-diameter BHI or standard slow-killing (SK) plates (modified NGM agar plates (0.35% instead of 0.25% peptone)) as indicated. The plates were then incubated overnight at 37°C. The plates were cooled to room temperature for at least 30 min before seeding with animals. Synchronized young gravid adult hermaphroditic animals grown on *E. coli* OP50 were transferred outside the indicated bacterial lawns, and the numbers of animals on and off the lawns were counted at the specified times for each experiment. Three

bioRxiv preprint doi: https://doi.org/10.1101/2020.12.18.423492; this version posted December 19, 2020. The copyright holder for this preprint (which was not certified by peer review) is the author/funder, who has granted bioRxiv a license to display the preprint in perpetuity. It is made available under aCC-BY-NC-ND 4.0 International license.

3.5-cm-diameter plates were used per trial in every experiment. Occupancy index was calculated as (N_{on} lawn/N_{total}). For first exiting events, individual animals were monitored and the time that the animal first left the lawn was recorded. For exploratory events entry and exiting events were recorded for 10 minutes at 50 minutes and 3 hours and 50 minutes after transfer.

Avoidance assays at 8% oxygen

Avoidance assays as described above were carried out in a hypoxia chamber. Briefly, after young gravid adult hermaphroditic animals were transferred to the avoidance plates, the plates were placed in the hypoxia chamber and the lids of the plates were removed. The chamber was purged with 8% oxygen (balanced with nitrogen) for 5 min at a flow rate of 25 L/min. The chamber was then sealed and assays were carried out. Control plates were incubated at ambient oxygen.

Avoidance assays with bacterial RNA

RNA from bacterial pellets was isolated and used for avoidance assays as previously described (Kaletsky et al., 2020). Briefly, bacteria for RNA collection were grown on SK or BHI plates overnight at 37°C. Bacterial lawns were collected from the surface of the plates using 1 mL of M9 buffer and a cell scraper. The resulting suspension was transferred to a 15-mL conical tube. PA14, OG1RF, or OP50 from 15 lawns was pooled in each tube and pelleted at 5,000g for 10 min at 4°C. The supernatant was discarded and the pellet was resuspended in 1 mL of Trizol LS for every 100-µL of bacterial pellet recovered. The pellet was resuspended by vortexing and subsequently frozen at -80°C until RNA isolation. 240 µg of total RNA was placed directly onto OP50 lawns and allowed to dry at room temperature before transferring worms over for avoidance assays.

Aversive training

3.5-cm-diameter training plates containing either *E. coli* OP50 on SK agar or *E. faecalis* OG1RF on BHI agar were made as described above for avoidance assays. For RNA training assays, SK plates containing *E. coli* OP50 were spotted with the appropriate isolated RNA. Young gravid adult hermaphroditic animals grown on *E. coli* OP50 were transferred to the training plates and allowed to roam for 4 hours for *E. faecalis* training or 24 hours for RNA training. They were then transferred to the appropriate assay plates.

Two-choice preference assays

Bacterial cultures were grown as indicated in the lawn avoidance assays above. Then, 20-µL of each inoculum was plated on opposite sides of a 6-cm-diameter BHI or SK plate and incubated overnight at 37°C. The plates were cooled to room temperature for at least 30 min before

bioRxiv preprint doi: https://doi.org/10.1101/2020.12.18.423492; this version posted December 19, 2020. The copyright holder for this preprint (which was not certified by peer review) is the author/funder, who has granted bioRxiv a license to display the preprint in perpetuity. It is made available under aCC-BY-NC-ND 4.0 International license.

seeding with animals. For the "Paralyzed" condition, 1 µL of 1M sodium azide was spotted onto each bacterial lawn. Young gravid adult hermaphroditic animals grown on *E. coli* OP50 were transferred to the center of plates equidistant from both the lawns. The numbers of animals on both lawns were counted at the specified times for each experiment. Three 6-cm-diameter plates were used per trial in every experiment. The *E. faecalis* choice index (*E. faecalis* CI) was calculated as follows:

$$E.faecalis\ \mathrm{CI} = \frac{[(\mathrm{No.\ of\ worms\ on}\ E.faecalis) - (\mathrm{No.\ of\ worms\ on}\ E.coli)]}{[(\mathrm{No.\ of\ worms\ on}\ E.faecalis) + (\mathrm{No.\ of\ worms\ on}\ E.coli)]}$$

Choice indices to other bacteria were similarly calculated.

Two-choice odor preference assays (lid choice assays)

A modified version of the two-choice preference assays was carried out as previously described (Worthy et al., 2018) to assess odor preference alone. To do this, bacterial cultures were grown and plated as indicated in the two-choice preference assays above. Then, agar plugs with the bacterial lawns were cut from the plates and transferred to the lids of new 6-cm-diameter BHI agar plates without any bacteria so that the bacteria on the agar plugs faced down towards the plate surface on opposite sides of the plate. 2 µL of 1M sodium azide was spotted on the surface below each agar plug. Young gravid adult hermaphroditic animals grown on *E. coli* OP50 (naïve) or from *E. faecalis* OG1RF training plates were transferred to the center of plates equidistant from both agar plugs. The numbers of animals paralyzed under each agar plug were counted after one hour. Three 6-cm-diameter plates were used per trial in every experiment. The choice index was calculated as indicated above.

Dry Drop Assay

The dry drop assay was carried out as previously described (Tran et al., 2017). Using a capillary, a dry drop of either SDS (positive control), BHI or LB (negative control), or *E. faecalis* or *E. faecium* cultures was placed on a dry SK plate in front of a forward-moving animal. A response was counted if an animal initiated backward movement. Response Index = Number of Responses / Total Number of Drops.

Imaging and quantification

Fluorescence imaging was carried out as described previously (Singh and Aballay, 2017) with slight modifications. Briefly, the animals were anesthetized using an M9 salt solution containing 50 mM sodium azide and mounted onto 2% agar pads. The animals were then visualized using a Leica M165 FC fluorescence stereomicroscope. For quantification of intestinal lumen bloating, brightfield images were acquired at each time point using the Leica LAS v4.6 software and the diameter of the intestinal lumen was measured using ImageJ software. For quantification of

bioRxiv preprint doi: https://doi.org/10.1101/2020.12.18.423492; this version posted December 19, 2020. The copyright holder for this preprint (which was not certified by peer review) is the author/funder, who has granted bioRxiv a license to display the preprint in perpetuity. It is made available under aCC-BY-NC-ND 4.0 International license.

fluorescent immune reporters, fluorescent images were acquired using the Leica LAS v4.6 software in greyscale as presented, and the fluorescence intensity was measured and averaged across three points in the intestine of each animal at the indicated time points using ImageJ software.

Statistical analysis

The statistical analysis was performed with Prism 8 (GraphPad). For box-and-whisker plots, the center line depicts the median and the box range depicts the first and third quartile, while the whiskers depict the minimum and maximum data points. For all box plots, individual dots represent individual trials. For time course figures, the mean and standard deviation of 9 trials is depicted at each time point. All experiments were performed in triplicate on three separate days. Unpaired t-tests, One-way or two-way ANOVA with subsequent group comparisons were performed as indicated in the figure legends. In the figures, ns denotes not significant and asterisks (*) denote statistical significance as follows: *, $p \leq 0.05$; **, $p \leq 0.01$; ***, $p \leq 0.001$; ****, $p \leq 0.0001$, as compared with the appropriate controls.

ACKNOWLEDGEMENTS

We thank Danielle A. Garsin (McGovern Medical School) for providing the *E. faecalis* OG1RF *ΔfsrB* and GFP strains. Some strains used in this study were provided by the Caenorhabditis Genetics Center (CGC), which is funded by the NIH Office of Research Infrastructure Programs (P40OD01044). Images were created using Microsoft PowerPoint and BioRender.com.

FIGURE LEGENDS

Figure 1. *E. faecalis* elicits fast avoidance in *C. elegans*. **(A)** Schematic of avoidance assays (top) and representative photomicrographs (bottom) of *C. elegans* on lawns of *E. coli* OP50, *P. aeruginosa* PA14, or *E. faecalis* OG1RF at 0 hours (left) and 4 hours (right) on BHI media. Individual animals are outlined in red. Scale bar, 5 mm. **(B)** Occupancy index of N2 animals after 4 hours of incubation on *E. coli*, *P. aeruginosa*, *E. faecalis*, *E. faecium*, or *S. aureus*. One-way ANOVA with subsequent comparison to *E. coli* as the control group was performed. Occupancy Index = (Number of animals on bacterial lawn) / (Total Number of animals). **(C)** Individual animals were tracked on lawns of *E. faecalis* and the time that they first left the lawn after transfer was recorded. Wild-type (WT, N2 Bristol) animals showed an average first leave time of 19.20 minutes while *tax-2(p671)* animals showed an average first leave time of 61.98 minutes. An unpaired t-test between the groups was performed. **(D)** N2 animals on standard avoidance assays plates with *E. faecalis* were observed for 10 minutes during two different time windows (0-1 hours and 3-4 hours) and the number of times the animals left and entered the bacteria lawns was counted. One-way ANOVA with subsequent comparisons between all groups was performed. **(E)** Occupancy index of N2 animals after 24-hour incubation on *P. aeruginosa* PA14

bioRxiv preprint doi: https://doi.org/10.1101/2020.12.18.423492; this version posted December 19, 2020. The copyright holder for this preprint (which was not certified by peer review) is the author/funder, who has granted bioRxiv a license to display the preprint in perpetuity. It is made available under aCC-BY-NC-ND 4.0 International license.

lawns or *E. coli* OP50 lawns supplemented with isolated total RNA from *E. coli* (*E.c.* RNA), *P. aeruginosa* (*P.a.* RNA), or *E. faecalis* (*E.f.* RNA). One-way ANOVA with subsequent comparison to *E. coli* RNA as the control group was performed.

Figure 2: Anterior intestinal distention elicits avoidance of *E. faecalis.* **(A)** Representative photomicrographs of animals at 4 hours on BHI media with *E. coli* (left), *P. aeruginosa* (middle), or *E. faecalis* (right). Red arrows point to the borders of the anterior intestine while blue arrows point the borders of the medial intestine. **(B)** Quantification of the anterior (top) and medial (bottom) intestinal lumen diameter of animals on *E. coli*, *P. aeruginosa*, or *E. faecalis* at 1, 2, and 4 hours. Two-way ANOVA was performed with comparison to the *E. coli* group at each timepoint. **(C)** Representative photomicrographs with fluorescent and brightfield images merged of *E. coli, P. aeruginosa*, and *E. faecalis* expressing GFP in the intestinal lumen of animals at 4 hours. **(D)** Occupancy index on *E. faecalis* at 4 hours of WT animals compared to either RNAi-mediated knockdown of *nol-6* or a loss-of-function mutation in *nol-6*. One-way ANOVA was performed with subsequent comparison to the WT group as the control. **(E)** A representative photomicrograph of a *nol-6(ac1)* animal after exposure to *E. faecalis* for 4 hours. Red arrows point to the borders of the anterior intestine and blue arrows point to the borders of the medial intestine. **(F)** Quantification of anterior and medial intestinal lumen diameter of *nol-6(ac1)* animals at 0 and 4 hours on *E. faecalis*. Two-way ANOVA was performed with comparison to the 0-hour groups for both anterior and medial quantifications.

Figure 3. Avoidance of *E. faecalis* is independent of virulence. **(A)** Occupancy index of N2 animals on virulent *E. faecalis* OG1RF and avirulent *E. faecalis* OG1RF *ΔfsrB* at 4 hours. An unpaired t-test was performed. **(B)** Representative fluorescent micrographs of *clec-60p::GFP* (top) and *ilys-3p::GFP* (bottom) animals at 0, 4, and 24 hours on *E. faecalis*. Scale bar, 200 µm. **(C)** Quantification of *clec-60::GFP* at 0, 4, and 24 hours on *E. faecalis*. One-way ANOVA was performed with comparisons to the 0-hour group as the control. **(D)** Quantification of *ilys-3p::GFP* at 0, 4, and 24 hours on *E. faecalis*. One-way ANOVA was performed with comparisons to the 0-hour group as the control.

Figure 4. NPR-1 and TAX-2/4 pathways regulate avoidance of *E. faecalis* and *P. aeruginosa*. **(A)** Occupancy index of WT animals compared to *npr-1(ad609)* and *npr-1(ok1447)* after 4 hours on *E. faecalis.* One-way ANOVA with subsequent comparison to WT animals as the control group was performed. **(B)** Occupancy index of WT, *npr-1(ad609)* and *npr-1(ok1447)* on lawns of *E. faecalis* in atmospheric oxygen or a chamber containing 8% oxygen. Two-way ANOVA with subsequent comparison to WT animals of each respective oxygen condition was performed. **(C)** Occupancy index of WT, *npr-1(ad609),* and *npr-1(ok1447)* in an 8% oxygen chamber at 1, 2, 3, and 4 hours, and 1 hour after removal from the chamber (vertical dashed line). Two-way ANOVA with subsequent comparison at each time point to WT animals was performed. **(D)** Occupancy index for WT and double loss-of-function mutants for *gcy-35*, *tax-2*, or *tax-4* and

bioRxiv preprint doi: https://doi.org/10.1101/2020.12.18.423492; this version posted December 19, 2020. The copyright holder for this preprint (which was not certified by peer review) is the author/funder, who has granted bioRxiv a license to display the preprint in perpetuity. It is made available under aCC-BY-NC-ND 4.0 International license.

npr-1 on *E. faecalis* for 4 hours and *P. aeruginosa* for 24 hours. Two-way ANOVA with subsequent comparisons to WT animals for each bacterium were performed. **(E)** Diagram of the neurons affected by *tax-2(p694)* and *tax-4(p678)*. The latter allele covers all *tax-2* expressing sensory neurons, while the former covers a subset. **(F)** Occupancy index for WT and single loss-of-function mutants for *tax-2* or *tax-4* on *E. faecalis* for 4 hours and *P. aeruginosa* for 24 hours. Two-way ANOVA as in with subsequent comparisons to WT animals for each bacterium were performed.

Figure 5. ASE, AWB, and AWC neurons mediate avoidance of *E. faecalis*. **(A)** Occupancy index on *E. faecalis* at 4 hours for WT, *tax-2(p694)* and animals with *tax-2* expression in ASE neurons (*flp-6p::tax-2*) or AQR, PQR, or URX neurons (*gcy-32p::tax-2*) in the *tax-2(p694)* background. One-way ANOVA with subsequent comparison to wild-type (WT) animals was performed. **(B)** Occupancy index of WT animals and animals with ablated neurons on *E. faecalis* at 4 hours and *P. aeruginosa* at 24 hours. Ablation of sensory neurons either by mutation (*che-1(p680)* = ASE(-)) or caspase expression (*sra-6p::mCasp-1* = ASH(-); *gpa-4p::TU#813 + gcy-27p::TU#814* = ASI(-); *str-1p::mCasp-1* = AWB(-); *ceh-36p::TU#813 + ceh-36p::TU#814* = AWC(-)). Two-way ANOVA with subsequent comparisons to WT groups for each respective bacterium were performed. **(C)** Occupancy index at 1 hour for WT and ASI(-) animals on *P. aeruginosa* lawns. Animals were trained on *E. coli* OP50 lawns supplemented with either *E. coli* or *P. aeruginosa* RNA for 24 hours Two-way ANOVA with subsequent comparison with WT control groups was performed. **(D)** Choice index after 1 hour for WT and ASI(-) animals choosing between *E. coli* and *P. aeruginosa* lawns. Two-way ANOVA with subsequent comparison with WT control groups was performed. Choice Index = (Number of animals on *E. coli* – Number of animals on *P. aeruginosa*) / (Number of animals on *E. coli* + Number of animals on *P. aeruginosa*). **(E)** Model for avoidance of *P. aeruginosa* (top) and *E. faecalis* (bottom) Avoidance of *P. aeruginosa* depends on both an ASI neuron-mediated bacterial sRNA pathway along with intestine-wide distention. The latter requires the NPR-1-dependent hyperoxia avoidance pathway along with AWB and AWC olfactory neurons. Avoidance of *E. faecalis* also depends on intestinal distention, though this is confined to the anterior intestine. This anterior intestinal distention-induced avoidance also requires NPR-1-dependent hyperoxia avoidance and AWB and AWC olfactory neurons, but also requires ASE chemosensory neurons.

Figure 6. AWB and AWC neurons are necessary for aversive olfactory learning following ingestion of *E. faecalis*. **(A)** Schematic of the choice assay (top) and quantification (bottom) of choice index for N2 animals choosing between *E. coli* and *E. faecalis* lawns and either free to move for 1 hour (Free to move) or paralyzed upon arrival at a bacterial lawn (Paralyzed). An unpaired t-test between the groups was performed. **(B)** Schematic of the lid choice assay (top) and quantification of naïve and trained choice index (bottom, left) and learning index (bottom, right) for WT, *tax-4(p678), tax-2(p671), tax-2(p694),* AWB(-), and AWC(-) animals. To train

bioRxiv preprint doi: https://doi.org/10.1101/2020.12.18.423492; this version posted December 19, 2020. The copyright holder for this preprint (which was not certified by peer review) is the author/funder, who has granted bioRxiv a license to display the preprint in perpetuity. It is made available under aCC-BY-NC-ND 4.0 International license.

animals, young adult animals were placed on *E. faecalis* lawns for 4 hours before the choice assay was performed. For choice index, two-way ANOVA with subsequent comparisons to the naïve and trained WT groups as controls were performed. For learning index, one-way ANOVA with comparison to the WT group as control was performed. Learning index = (Naïve choice index) – (Trained choice index).

Figure 7. The TRPM channels GON-2 and GTL-2 are required for distention-induced pathogen avoidance. **(A)** Occupancy index for wild-type, *gtl-2(n2618), gon-2(q362), gon-2(q388),* and *glp-1(e2141)* animals on *E. faecalis* at 4 hours or *P. aeruginosa* at 24 hours. Animals were grown to the young adult stage at 15°C. Two-way ANOVA with comparisons to the respective WT group for each bacterium were performed. **(B)** Occupancy index for wild-type, *gtl-2(n2618), gon-2(q362), gon-2(q388),* and *glp-1(e2141)* animals on *E. faecalis* at 4 hours or *P. aeruginosa* at 24 hours. Animals were grown to the young adult stage at 25°C. Two-way ANOVA with comparisons to the respective WT group for each bacterium were performed. **(C)** Occupancy index for WT, *gon-2(q388)* and *gtl-2(n2618)* animals with either RNAi-mediated knockdown of *aex-5* or an empty vector (EV) control on the *E. coli* HT115 lawns these animals were raised on. Two-way ANOVA with subsequent comparison between all groups was performed. **(D)** Occupancy index for WT, *gon-2(q388)* and *gtl-2(n2618)* animals with either RNAi-mediated knockdown of *aex-5* or an EV control on *E. faecalis* lawns at 4 hours. Two-way ANOVA with subsequent comparison between all groups was performed. **(E)** Model for avoidance of *P. aeruginosa* (top) and *E. faecalis* (bottom), as in **Figure 5E**, with the addition of a germline role in avoidance of *P. aeruginosa*, GON-2 and GTL-2 regulation of avoidance of *E. faecalis*, and the contribution of odor sensing pathways to avoidance for avoidance of both bacteria.

Figure 1 – Supplement 1. Avoidance of Gram-positive pathogens. **(A)** Occupancy index time course of N2 animals on either *E. faecalis*, *E. faecium*, or *S. aureus*. **(B)** Response index of N2 animals to dry drops of *E. coli*, *E. faecalis*, *E. faecium*, BHI, LB, or 0.6mM SDS buffer. Response Index = Number of Responses / Total Number of Drops.

Figure 2 – Supplement 2. *E. faecalis* but not *P. aeruginosa* causes anterior intestinal distention in *nol-6* animals**. (A)** Quantification of anterior and medial intestinal lumen diameter of *nol-6(ac1)* animals after 0 and 24 hours on *P. aeruginosa.* **(B)** Occupancy index of WT and *nol-6(ac1)* animals on *P. aeruginosa* at 24 hours. An unpaired t-test was performed. **(C)** Quantification of anterior intestinal lumen diameter of *nol-6* RNAi animals at 0 and 4 hours on *E. faecalis*. An unpaired t-test was performed. **(D)** Quantification of medial intestinal lumen diameter of *nol-6* RNAi animals at 0 and 4 hours on *E. faecalis*. An unpaired t-test was performed.

Figure 4 –Supplement 1. The TRPV subunits OCR-2 and OSM-9 slightly speed up avoidance of *E. faecalis*. **(A)** Occupancy index of WT animals compared to *ocr-2(ak47)* and *osm-9(yz6)* animals on *E. faecalis* at 4 hours. One-way ANOVA with subsequent comparison to WT animals was

bioRxiv preprint doi: https://doi.org/10.1101/2020.12.18.423492; this version posted December 19, 2020. The copyright holder for this preprint (which was not certified by peer review) is the author/funder, who has granted bioRxiv a license to display the preprint in perpetuity. It is made available under aCC-BY-NC-ND 4.0 International license.

performed. **(B)** Occupancy index time course for WT animals compared to *ocr-2(ak47)* and *osm-9(yz6)* on *E. faecalis*. Two-way ANOVA with comparison to WT animals at each time point was performed.

Figure 7 – Supplement 1. Screening TRP channels for effect on avoidance of *E. faecalis*. Occupancy index of WT animals on *E. faecalis* at 4 hours compared to 5 different TRP channel mutants: *gon-2(q362)*, *gon-2(q388)*, *gtl-2(n2618)*, and *gtl-2(tm1643)*. One-way ANOVA with subsequent comparison to WT animals was performed.

ADDITIONAL INFORMATION

Funding

This work was supported by a National Institute of General Medical Sciences grant (GM070907) and a National Institute of Allergy and Infectious Diseases grant (AI11791) to Alejandro Aballay.

Author contributions

Adam Filipowicz, Conceptualization, Data curation, Formal analysis, Investigation, Methodology, Writing – original draft, Writing – review and editing; Alejandro Aballay, Conceptualization, Data curation, Formal analysis, Funding acquisition, Writing – original draft, Project administration, Writing – review and editing

REFERENCES

Anderson, A., and McMullan, R. (2018). Neuronal and non-neuronal signals regulate *Caenorhabditis elegans* avoidance of contaminated food. Philos. Trans. R. Soc. B Biol. Sci. *373*.

Austin, J., and Kimble, J. (1987). *glp-1* is required in the germ line for regulation of the decision between mitosis and meiosis in *C. elegans*. Cell *51*, 589–599.

de Bono, M., and Bargmann, C.I. (1998). Natural variation in a neuropeptide Y receptor homolog modifies social behavior and food response in *C. elegans*. Cell *94*, 679–689.

de Bono, M., Tobin, D.M., Davis, M.W., Avery, L., and Bargmann, C.I. (2002). Social feeding in *Caenorhabditis elegans* is induced by neurons that detect aversive stimuli. Nature *419*, 899–903.

Bretscher, A.J., Kodama-Namba, E., Busch, K.E., Murphy, R.J., Soltesz, Z., Laurent, P., and de Bono, M. (2011). Temperature, Oxygen, and Salt-Sensing Neurons in *C. elegans* Are Carbon Dioxide Sensors that Control Avoidance Behavior. Neuron *69*, 1099–1113.

Cao, X., Kajino-Sakamoto, R., Doss, A., and Aballay, A. (2017). Distinct Roles of Sensory Neurons in Mediating Pathogen Avoidance and Neuropeptide-Dependent Immune Regulation. Cell Rep. *21*, 1442–1451.

bioRxiv preprint doi: https://doi.org/10.1101/2020.12.18.423492; this version posted December 19, 2020. The copyright holder for this preprint (which was not certified by peer review) is the author/funder, who has granted bioRxiv a license to display the preprint in perpetuity. It is made available under aCC-BY-NC-ND 4.0 International license.

Chalasani, S.H., Chronis, N., Tsunozaki, M., Gray, J.M., Ramot, D., Goodman, M.B., and Bargmann, C.I. (2007). Dissecting a circuit for olfactory behaviour in *Caenorhabditis elegans*. Nature *450*, 63–70.

Chalasani, S.H., Kato, S., Albrecht, D.R., Nakagawa, T., Abbott, L.F., and Bargmann, C.I. (2010). Neuropeptide feedback modifies odor-evoked dynamics in *Caenorhabditis elegans* olfactory neurons. Nat. Neurosci. *13*, 615–621.

Chang, A.J., Chronis, N., Karow, D.S., Marletta, M.A., and Bargmann, C.I. (2006). A Distributed Chemosensory Circuit for Oxygen Preference in *C. elegans*. PLOS Biol. *4*, e274.

Chen, Z., Hendricks, M., Cornils, A., Maier, W., Alcedo, J., and Zhang, Y. (2013). Two Insulin-like Peptides Antagonistically Regulate Aversive Olfactory Learning in *C. elegans*. Neuron *77*, 572–585.

Cheung, B.H.H., Arellano-Carbajal, F., Rybicki, I., and Bono, M. de (2004). Soluble Guanylate Cyclases Act in Neurons Exposed to the Body Fluid to Promote *C. elegans* Aggregation Behavior. Curr. Biol. *14*, 1105–1111.

Coates, J.C., and de Bono, M. (2002). Antagonistic pathways in neurons exposed to body fluid regulate social feeding in *Caenorhabditis elegans*. Nature *419*, 925–929.

Coburn, C.M., and Bargmann, C.I. (1996). A Putative Cyclic Nucleotide–Gated Channel Is Required for Sensory Development and Function in *C. elegans*. Neuron *17*, 695–706.

Crittenden, S.L., Troemel, E.R., Evans, T.C., and Kimble, J. (1994). GLP-1 is localized to the mitotic region of the *C. elegans* germ line. Dev. Camb. Engl. *120*, 2901–2911.

Engelmann, I., Griffon, A., Tichit, L., Montañana-Sanchis, F., Wang, G., Reinke, V., Waterston, R.H., Hillier, L.W., and Ewbank, J.J. (2011). A Comprehensive Analysis of Gene Expression Changes Provoked by Bacterial and Fungal Infection in *C. elegans*. PLoS ONE *6*.

Fadda, M., Fruyt, N.D., Borghgraef, C., Watteyne, J., Peymen, K., Vandewyer, E., Galindo, F.J.N., Kieswetter, A., Mirabeau, O., Chew, Y.L., et al. (2020). NPY/NPF-Related Neuropeptide FLP-34 Signals from Serotonergic Neurons to Modulate Aversive Olfactory Learning in *Caenorhabditis elegans*. J. Neurosci. *40*, 6018–6034.

Flavell, S.W., Pokala, N., Macosko, E.Z., Albrecht, D.R., Larsch, J., and Bargmann, C.I. (2013). Serotonin and the Neuropeptide PDF Initiate and Extend Opposing Behavioral States in *C. elegans*. Cell *154*, 1023–1035.

Fraser, A.G., Kamath, R.S., Zipperlen, P., Martinez-Campos, M., Sohrmann, M., and Ahringer, J. (2000). Functional genomic analysis of *C. elegans* chromosome I by systematic RNA interference. Nature *408*, 325–330.

bioRxiv preprint doi: https://doi.org/10.1101/2020.12.18.423492; this version posted December 19, 2020. The copyright holder for this preprint (which was not certified by peer review) is the author/funder, who has granted bioRxiv a license to display the preprint in perpetuity. It is made available under aCC-BY-NC-ND 4.0 International license.

Fuhrman, L.E., Goel, A.K., Smith, J., Shianna, K.V., and Aballay, A. (2009). Nucleolar Proteins Suppress *Caenorhabditis elegans* Innate Immunity by Inhibiting p53/CEP-1. PLoS Genet. *5*.

Garsin, D.A., Sifri, C.D., Mylonakis, E., Qin, X., Singh, K.V., Murray, B.E., Calderwood, S.B., and Ausubel, F.M. (2001). A simple model host for identifying Gram-positive virulence factors. Proc. Natl. Acad. Sci. *98*, 10892–10897.

Gravato-Nobre, M.J., Vaz, F., Filipe, S., Chalmers, R., and Hodgkin, J. (2016). The Invertebrate Lysozyme Effector ILYS-3 Is Systemically Activated in Response to Danger Signals and Confers Antimicrobial Protection in *C. elegans*. PLoS Pathog. *12*.

Gray, J.M., Karow, D.S., Lu, H., Chang, A.J., Chang, J.S., Ellis, R.E., Marletta, M.A., and Bargmann, C.I. (2004). Oxygen sensation and social feeding mediated by a *C. elegans* guanylate cyclase homologue. Nature *430*, 317–322.

Ha, H., Hendricks, M., Shen, Y., Gabel, C.V., Fang-Yen, C., Qin, Y., Colón-Ramos, D., Shen, K., Samuel, A.D.T., and Zhang, Y. (2010). Functional organization of a neural network for aversive olfactory learning in *Caenorhabditis elegans*. Neuron *68*, 1173–1186.

Harris, G., Shen, Y., Ha, H., Donato, A., Wallis, S., Zhang, X., and Zhang, Y. (2014). Dissecting the Signaling Mechanisms Underlying Recognition and Preference of Food Odors. J. Neurosci. *34*, 9389–9403.

Holzer, P. (2011). TRP channels in the digestive system. Curr. Pharm. Biotechnol. *12*, 24–34.

Irazoqui, J.E., Troemel, E.R., Feinbaum, R.L., Luhachack, L.G., Cezairliyan, B.O., and Ausubel, F.M. (2010). Distinct Pathogenesis and Host Responses during Infection of *C. elegans* by *P. aeruginosa* and *S. aureus*. PLoS Pathog. *6*.

Kaletsky, R., Moore, R.S., Vrla, G.D., Parsons, L.R., Gitai, Z., and Murphy, C.T. (2020). *C. elegans* interprets bacterial non-coding RNAs to learn pathogenic avoidance. Nature 1–7.

Kaplan, J.M., and Horvitz, H.R. (1993). A dual mechanosensory and chemosensory neuron in *Caenorhabditis elegans*. Proc. Natl. Acad. Sci. U. S. A. *90*, 2227–2231.

Kavaliers, M., Ossenkopp, K.-P., and Choleris, E. (2019). Social neuroscience of disgust. Genes Brain Behav. *18*, e12508.

Kindt, K.S., Viswanath, V., Macpherson, L., Quast, K., Hu, H., Patapoutian, A., and Schafer, W.R. (2007). *Caenorhabditis elegans* TRPA-1 functions in mechanosensation. Nat. Neurosci. *10*, 568–577.

Kiyama, Y., Miyahara, K., and Ohshima, Y. (2012). Active uptake of artificial particles in the nematode *Caenorhabditis elegans*. J. Exp. Biol. *215*, 1178–1183.

bioRxiv preprint doi: https://doi.org/10.1101/2020.12.18.423492; this version posted December 19, 2020. The copyright holder for this preprint (which was not certified by peer review) is the author/funder, who has granted bioRxiv a license to display the preprint in perpetuity. It is made available under aCC-BY-NC-ND 4.0 International license.

Kumar, S., Egan, B.M., Kocsisova, Z., Schneider, D.L., Murphy, J.T., Diwan, A., and Kornfeld, K. (2019). Lifespan Extension in *C. elegans* Caused by Bacterial Colonization of the Intestine and Subsequent Activation of an Innate Immune Response. Dev. Cell *49*, 100-117.e6.

Lee, K., and Mylonakis, E. (2017). An Intestine-Derived Neuropeptide Controls Avoidance Behavior in *Caenorhabditis elegans*. Cell Rep. *20*, 2501–2512.

Leinwand, S.G., and Chalasani, S.H. (2013). Neuropeptide signaling remodels chemosensory circuit composition in *Caenorhabditis elegans*. Nat. Neurosci. *16*, 1461–1467.

Leinwand, S.G., Yang, C.J., Bazopoulou, D., Chronis, N., Srinivasan, J., and Chalasani, S.H. (2015). Circuit mechanisms encoding odors and driving aging-associated behavioral declines in *Caenorhabditis elegans*. ELife *4*, e10181.

Medzhitov, R., Schneider, D.S., and Soares, M.P. (2012). Disease tolerance as a defense strategy. Science *335*, 936–941.

Meisel, J.D., and Kim, D.H. (2014). Behavioral avoidance of pathogenic bacteria by *Caenorhabditis elegans*. Trends Immunol. *35*, 465–470.

Meisel, J.D., Panda, O., Mahanti, P., Schroeder, F.C., and Kim, D.H. (2014). Chemosensation of Bacterial Secondary Metabolites Modulates Neuroendocrine Signaling and Behavior of *C. elegans*. Cell *159*, 267–280.

Metaxakis, A., Petratou, D., and Tavernarakis, N. (2018). Multimodal sensory processing in *Caenorhabditis elegans*. Open Biol. *8*.

Milward, K., Busch, K.E., Murphy, R.J., Bono, M. de, and Olofsson, B. (2011). Neuronal and molecular substrates for optimal foraging in *Caenorhabditis elegans*. Proc. Natl. Acad. Sci. *108*, 20672–20677.

Moore, R.S., Kaletsky, R., and Murphy, C.T. (2019). Piwi/PRG-1 Argonaute and TGF-β Mediate Transgenerational Learned Pathogenic Avoidance. Cell *177*, 1827-1841.e12.

Mueller-Tribbensee, S.M., Karna, M., Khalil, M., Neurath, M.F., Reeh, P.W., and Engel, M.A. (2015). Differential Contribution of TRPA1, TRPV4 and TRPM8 to Colonic Nociception in Mice. PLoS ONE *10*.

Mylonakis, E., Engelbert, M., Qin, X., Sifri, C.D., Murray, B.E., Ausubel, F.M., Gilmore, M.S., and Calderwood, S.B. (2002). The Enterococcus faecalis *fsrB* Gene, a Key Component of the fsr Quorum-Sensing System, Is Associated with Virulence in the Rabbit Endophthalmitis Model. Infect. Immun. *70*, 4678–4681.

Olofsson, B. (2014). The olfactory neuron AWC promotes avoidance of normally palatable food following chronic dietary restriction. J. Exp. Biol. *217*, 1790–1798.

bioRxiv preprint doi: https://doi.org/10.1101/2020.12.18.423492; this version posted December 19, 2020. The copyright holder for this preprint (which was not certified by peer review) is the author/funder, who has granted bioRxiv a license to display the preprint in perpetuity. It is made available under aCC-BY-NC-ND 4.0 International license.

Pradel, E., Zhang, Y., Pujol, N., Matsuyama, T., Bargmann, C.I., and Ewbank, J.J. (2007). Detection and avoidance of a natural product from the pathogenic bacterium *Serratia marcescens* by *Caenorhabditis elegans*. Proc. Natl. Acad. Sci. U. S. A. *104*, 2295–2300.

Reddy, K.C., Andersen, E.C., Kruglyak, L., and Kim, D.H. (2009). A Polymorphism in *npr-1* Is a Behavioral Determinant of Pathogen Susceptibility in *C. elegans*. Science *323*, 382–384.

Reddy, K.C., Hunter, R.C., Bhatla, N., Newman, D.K., and Kim, D.H. (2011). *Caenorhabditis elegans* NPR-1–mediated behaviors are suppressed in the presence of mucoid bacteria. Proc. Natl. Acad. Sci. U. S. A. *108*, 12887–12892.

Rogers, C., Reale, V., Kim, K., Chatwin, H., Li, C., Evans, P., and de Bono, M. (2003). Inhibition of *Caenorhabditis elegans* social feeding by FMRFamide-related peptide activation of NPR-1. Nat. Neurosci. *6*, 1178–1185.

Sarabian, C., Curtis, V., and McMullan, R. (2018). Evolution of pathogen and parasite avoidance behaviours†. Philos. Trans. R. Soc. B Biol. Sci. *373*.

Shtonda, B.B., and Avery, L. (2006). Dietary choice behavior in *Caenorhabditis elegans*. J. Exp. Biol. *209*, 89–102.

Sifri, C.D., Mylonakis, E., Singh, K.V., Qin, X., Garsin, D.A., Murray, B.E., Ausubel, F.M., and Calderwood, S.B. (2002). Virulence effect of *Enterococcus faecalis* protease genes and the quorum-sensing locus *fsr* in *Caenorhabditis elegans* and mice. Infect. Immun. *70*, 5647–5650.

Singh, J., and Aballay, A. (2017). Endoplasmic Reticulum Stress Caused by Lipoprotein Accumulation Suppresses Immunity against Bacterial Pathogens and Contributes to Immunosenescence. MBio *8*.

Singh, J., and Aballay, A. (2019a). Intestinal infection regulates behavior and learning via neuroendocrine signaling. ELife *8*, e50033.

Singh, J., and Aballay, A. (2019b). Microbial Colonization Activates an Immune Fight-and-Flight Response via Neuroendocrine Signaling. Dev. Cell *49*, 89-99.e4.

Singh, J., and Aballay, A. (2020). Neural control of behavioral and molecular defenses in *C. elegans*. Curr. Opin. Neurobiol. *62*, 34–40.

Soldano, A., Alpizar, Y.A., Boonen, B., Franco, L., López-Requena, A., Liu, G., Mora, N., Yaksi, E., Voets, T., Vennekens, R., et al (2016). Gustatory-mediated avoidance of bacterial lipopolysaccharides via TRPA1 activation in *Drosophila*. ELife *5*.

Stensmyr, M.C., Dweck, H.K.M., Farhan, A., Ibba, I., Strutz, A., Mukunda, L., Linz, J., Grabe, V., Steck, K., Lavista-Llanos, S., et al. (2012). A Conserved Dedicated Olfactory Circuit for Detecting Harmful Microbes in *Drosophila*. Cell *151*, 1345–1357.

bioRxiv preprint doi: https://doi.org/10.1101/2020.12.18.423492; this version posted December 19, 2020. The copyright holder for this preprint (which was not certified by peer review) is the author/funder, who has granted bioRxiv a license to display the preprint in perpetuity. It is made available under aCC-BY-NC-ND 4.0 International license.

Styer, K.L., Singh, V., Macosko, E., Steele, S.E., Bargmann, C.I., and Aballay, A. (2008). Innate Immunity in *Caenorhabditis elegans* Is Regulated by Neurons Expressing NPR-1/GPCR. Science *322*, 460–464.

Summers, P.J., Layne, R.M., Ortega, A.C., Harris, G.P., Bamber, B.A., and Komuniecki, R.W. (2015). Multiple Sensory Inputs Are Extensively Integrated to Modulate Nociception in *C. elegans*. J. Neurosci. *35*, 10331–10342.

Sun, A.Y., and Lambie, E.J. (1997). Gon-2, a Gene Required for Gonadogenesis in *Caenorhabditis elegans*. Genetics *147*, 1077–1089.

TeKippe, M., and Aballay, A. (2010). *C. elegans* Germline-Deficient Mutants Respond to Pathogen Infection Using Shared and Distinct Mechanisms. PLoS ONE *5*.

Teramoto, T., Lambie, E.J., and Iwasaki, K. (2005). Differential regulation of TRPM channels governs electrolyte homeostasis in the *C. elegans* intestine. Cell Metab. *1*, 343–354.

Teramoto, T., Sternick, L.A., Kage-Nakadai, E., Sajjadi, S., Siembida, J., Mitani, S., Iwasaki, K., and Lambie, E.J. (2010). Magnesium Excretion in *C. elegans* Requires the Activity of the GTL-2 TRPM Channel. PLOS ONE *5*, e9589.

Timmons, L., and Fire, A. (1998). Specific interference by ingested dsRNA. Nature *395*, 854–854.

Tran, A., Tang, A., O'Loughlin, C.T., Balistreri, A., Chang, E., Coto Villa, D., Li, J., Varshney, A., Jimenez, V., Pyle, J., et al. (2017). *C. elegans* avoids toxin-producing Streptomyces using a seven transmembrane domain chemosensory receptor. ELife *6*, e23770.

Wani, K.A., Goswamy, D., and Irazoqui, J.E. (2020). Nervous system control of intestinal host defense in *C. elegans*. Curr. Opin. Neurobiol. *62*, 1–9.

Wilson, M.A., Iser, W.B., Son, T.G., Logie, A., Cabral-Costa, J.V., Mattson, M.P., and Camandola, S. (2017). *skn-1* is required for interneuron sensory integration and foraging behavior in *Caenorhabditis elegans*. PLoS ONE *12*.

Worthy, S.E., Rojas, G.L., Taylor, C.J., and Glater, E.E. (2018). Identification of Odor Blend Used by *Caenorhabditis elegans* for Pathogen Recognition. Chem. Senses *43*, 169–180.

Xiao, R., and Xu, X.Z.S. (2011). *C. elegans* TRP channels. Adv. Exp. Med. Biol. *704*, 323–339.

Xiao, R., Zhang, B., Dong, Y., Gong, J., Xu, T., Liu, J., and Xu, X.Z.S. (2013). A Genetic Program Promotes *C. elegans* Longevity at Cold Temperatures via a Thermosensitive TRP Channel. Cell *152*, 806–817.

Yoshida, K., Hirotsu, T., Tagawa, T., Oda, S., Wakabayashi, T., Iino, Y., and Ishihara, T. (2012). Odour concentration-dependent olfactory preference change in *C. elegans*. Nat. Commun. *3*, 739.

bioRxiv preprint doi: https://doi.org/10.1101/2020.12.18.423492; this version posted December 19, 2020. The copyright holder for this preprint (which was not certified by peer review) is the author/funder, who has granted bioRxiv a license to display the preprint in perpetuity. It is made available under aCC-BY-NC-ND 4.0 International license.

Yuen, G.J., and Ausubel, F.M. (2018). Both live and dead *Enterococci* activate *Caenorhabditis elegans* host defense via immune and stress pathways. Virulence *9*, 683–699.

Zhang, Y., Lu, H., and Bargmann, C.I. (2005). Pathogenic bacteria induce aversive olfactory learning in *Caenorhabditis elegans*. Nature *438*, 179–184.

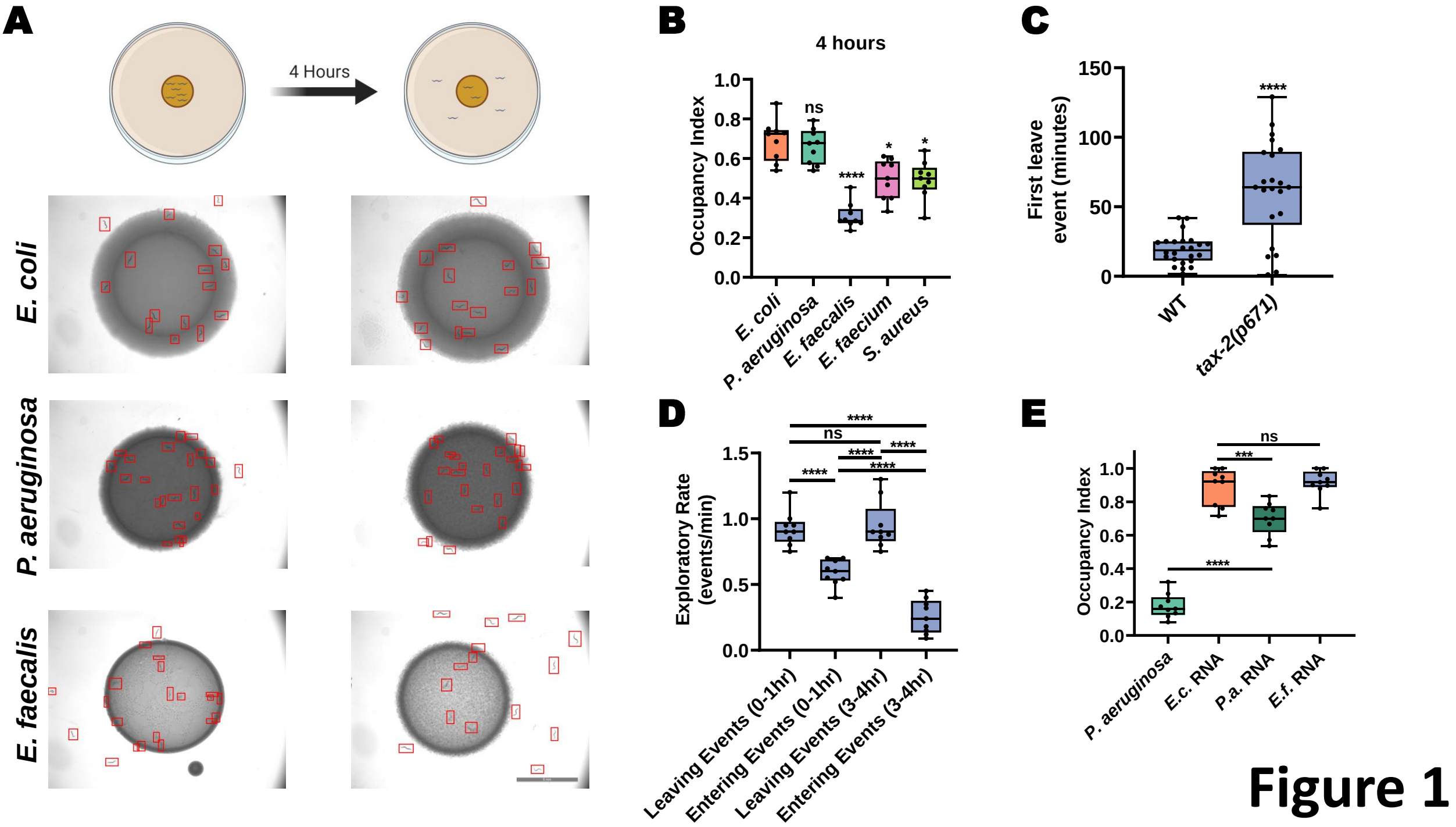
A
4 Hours
E. coli
P. aeruginosa
E. faecalis
B
4 hours
Occupancy Index
1.0
0.8
0.6
0.4
0.2
0.0
ns
****
*
*
E. coli
P. aeruginosa
E. faecalis
E. faecium
S. aureus
C
First leave event (minutes)
150
100
50
0
****
WT
tax-2(p671)
D
Exploratory Rate (events/min)
1.5
1.0
0.5
0.0
****
ns
****
****
****
****
Leaving Events (0-1hr)
Entering Events (0-1hr)
Leaving Events (3-4hr)
Entering Events (3-4hr)
E
Occupancy Index
1.0
0.8
0.6
0.4
0.2
0.0
ns
***
****
P. aeruginosa
E.c. RNA
P.a. RNA
E.f. RNA

Figure 1

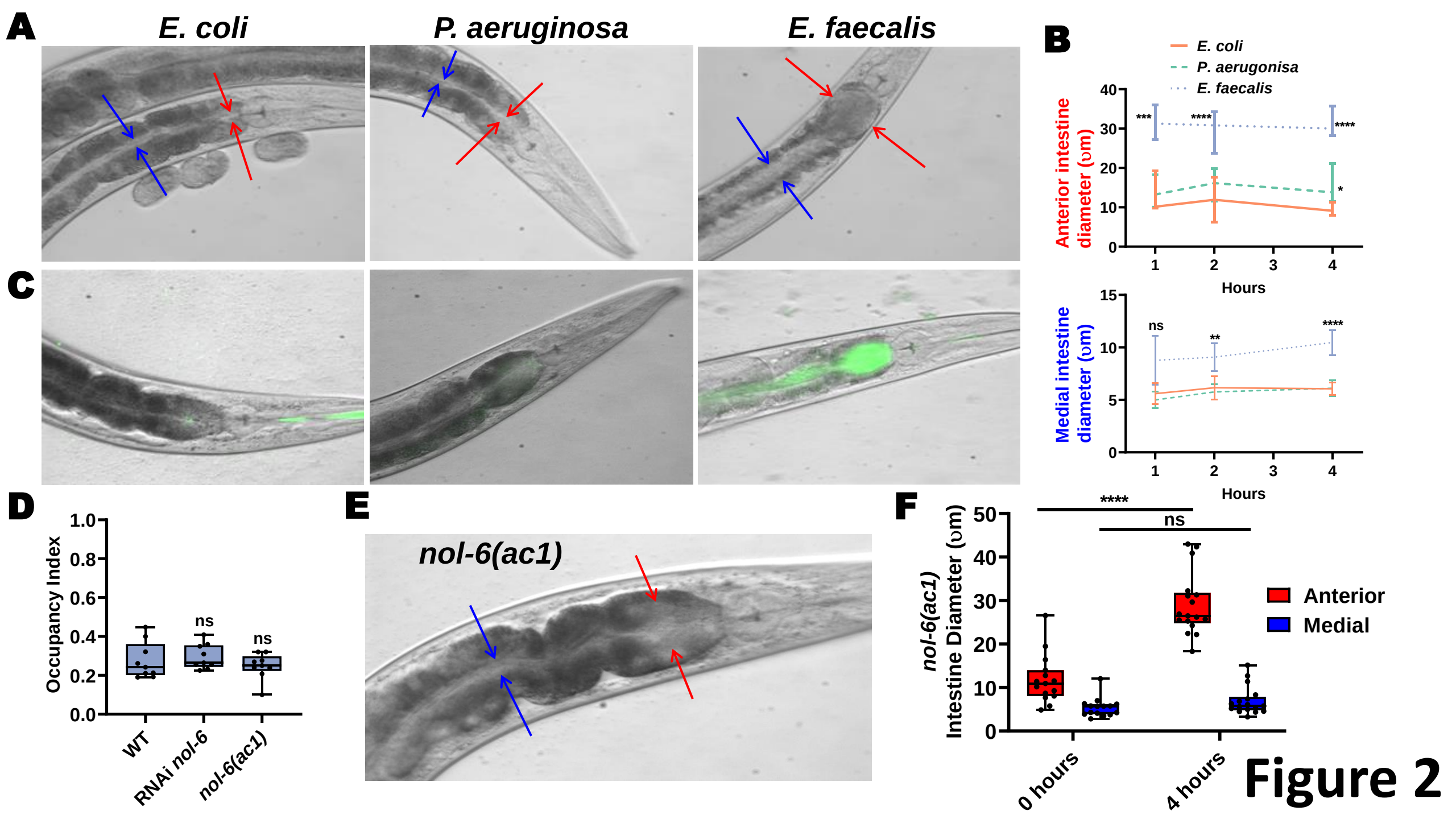
A
E. coli
P. aeruginosa
E. faecalis
B
E. coli
P. aerugonisa
E. faecalis
Anterior intestine diameter (υm)
Hours
Medial intestine diameter (υm)
Hours
C
D
Occupancy Index
ns
ns
WT
RNAi nol-6
nol-6(ac1)
E
nol-6(ac1)
F
nol-6(ac1) Intestine Diameter (υm)
****
ns
Anterior
Medial
0 hours
4 hours

Figure 2

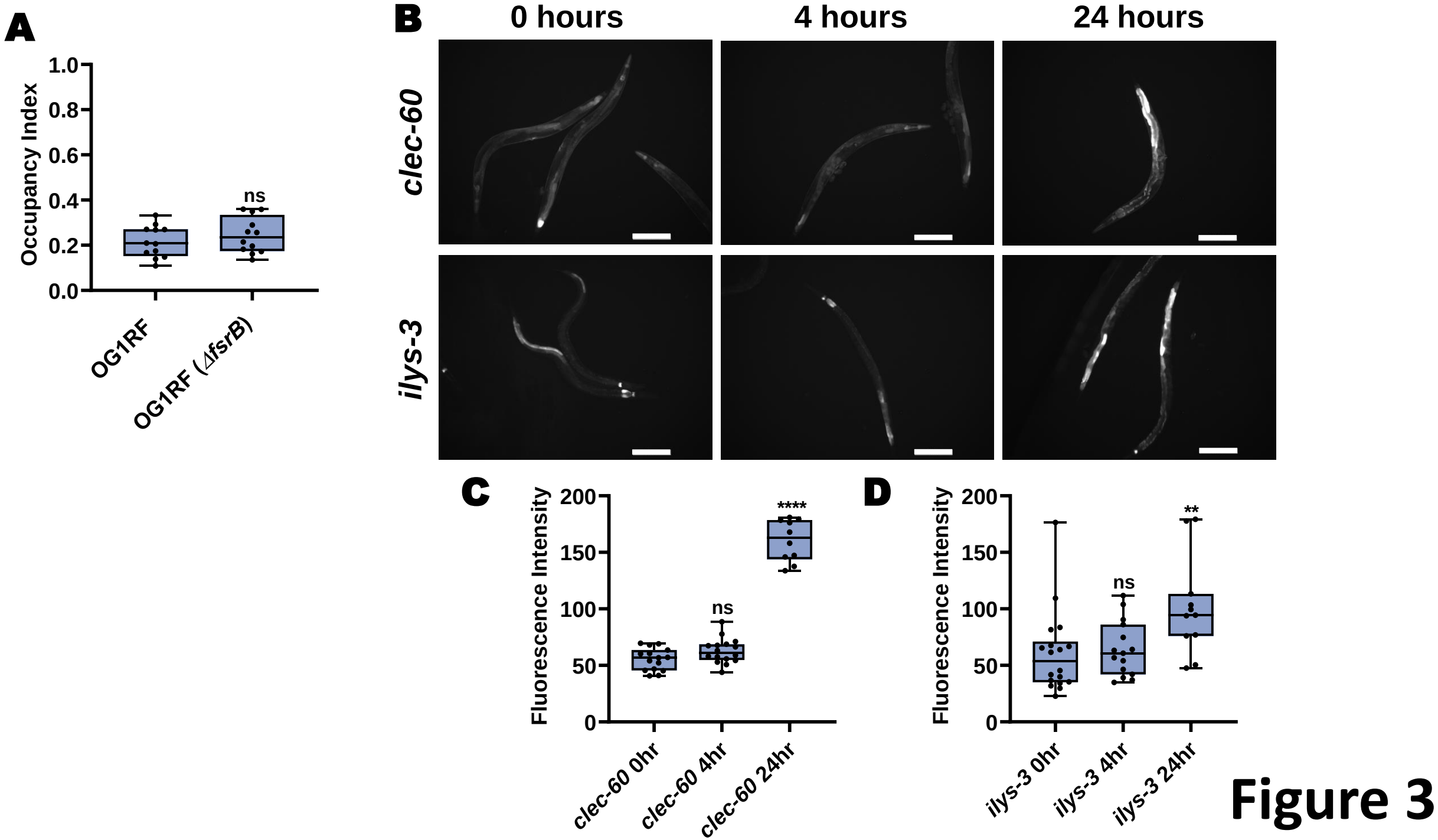
A
Occupancy Index
1.0
0.8
0.6
0.4
0.2
0.0
ns
OG1RF
OG1RF (ΔfsrB)
B
0 hours
4 hours
24 hours
clec-60
ilys-3
C
Fluorescence Intensity
200
150
100
50
0
****
ns
clec-60 0hr
clec-60 4hr
clec-60 24hr
D
Fluorescence Intensity
200
150
100
50
0
**
ns
ilys-3 0hr
ilys-3 4hr
ilys-3 24hr

Figure 3

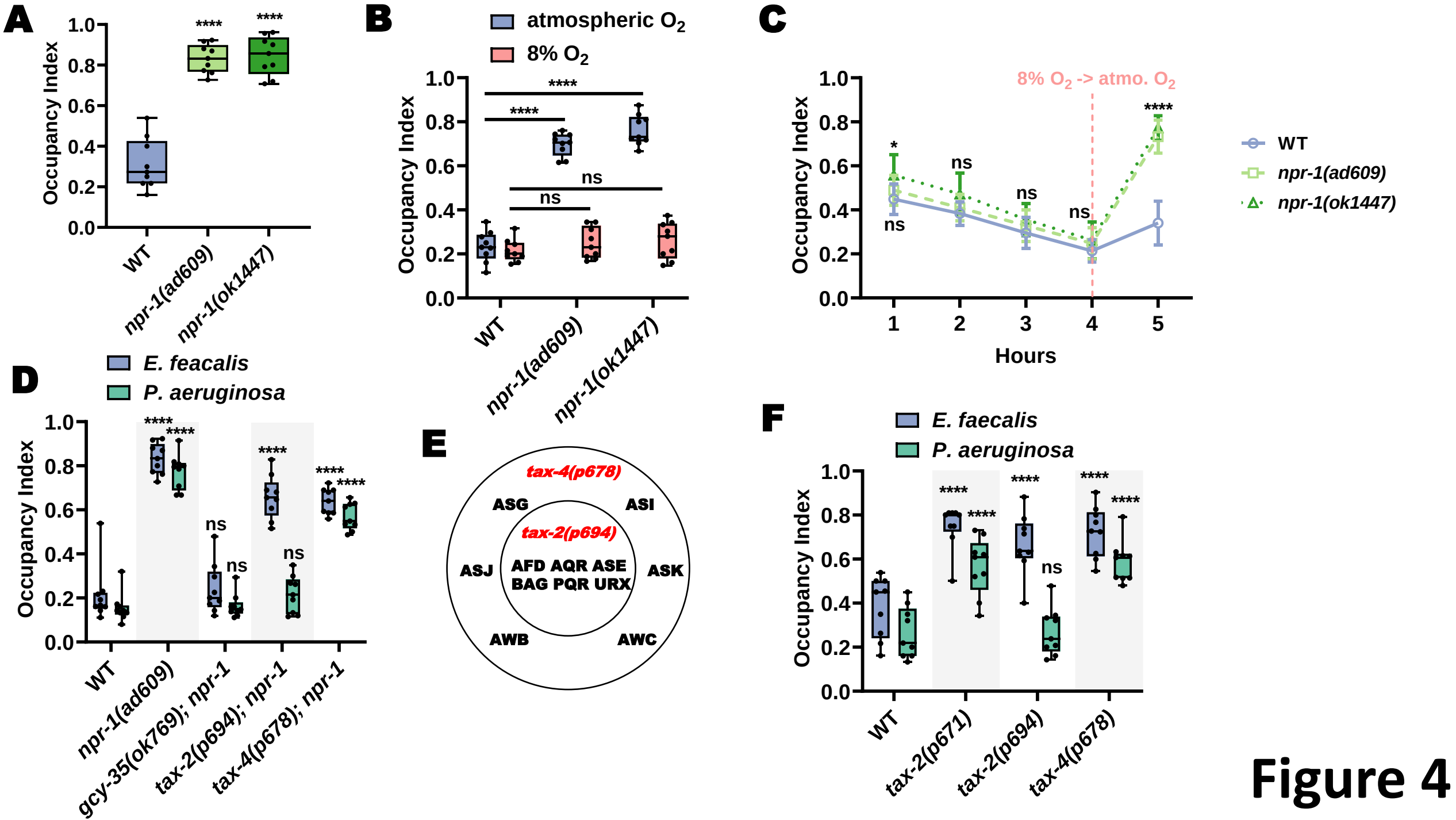
A
Occupancy Index
1.0
0.8
0.6
0.4
0.2
0.0
****
****
WT
npr-1(ad609)
npr-1(ok1447)
B
atmospheric O2
8% O2
Occupancy Index
****
****
ns
ns
WT
npr-1(ad609)
npr-1(ok1447)
C
8% O2 -> atmo. O2
Occupancy Index
*
ns
ns
ns
ns
****
1
2
3
4
5
Hours
WT
npr-1(ad609)
npr-1(ok1447)
D
E. feacalis
P. aeruginosa
Occupancy Index
****
****
ns
ns
****
ns
****
****
WT
npr-1(ad609)
gcy-35(ok769); npr-1
tax-2(p694); npr-1
tax-4(p678); npr-1
E
tax-4(p678)
ASG
ASI
tax-2(p694)
ASJ
AFD AQR ASE
BAG PQR URX
ASK
AWB
AWC
F
E. faecalis
P. aeruginosa
Occupancy Index
****
****
****
ns
****
****
WT
tax-2(p671)
tax-2(p694)
tax-4(p678)

Figure 4

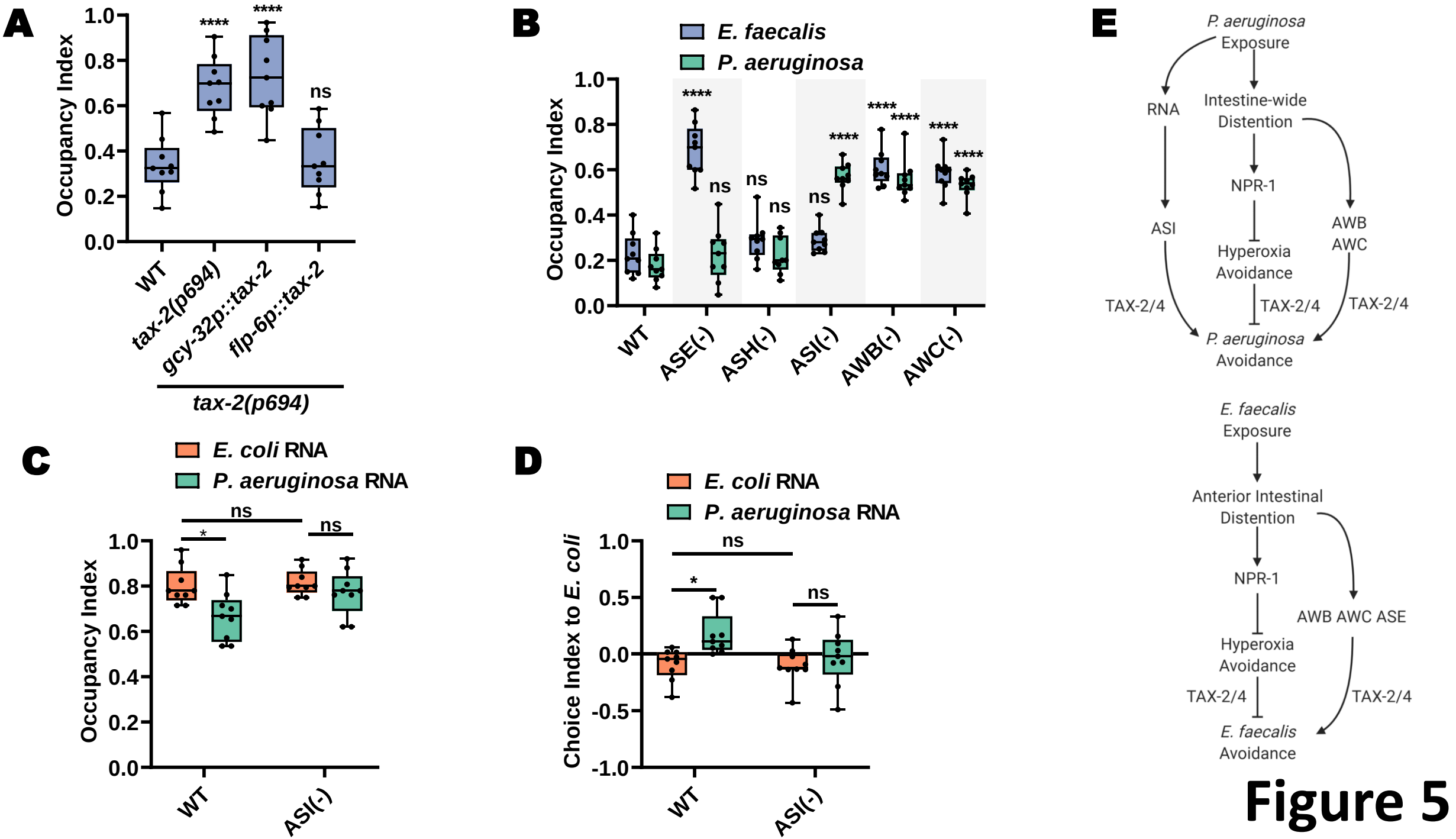
A
Occupancy Index
1.0
0.8
0.6
0.4
0.2
0.0
****
****
ns
WT
tax-2(p694)
gcy-32p::tax-2
flp-6p::tax-2
tax-2(p694)
B
E. faecalis
P. aeruginosa
Occupancy Index
WT
ASE(-)
ASH(-)
ASI(-)
AWB(-)
AWC(-)
C
E. coli RNA
P. aeruginosa RNA
Occupancy Index
ns
*
ns
WT
ASI(-)
D
E. coli RNA
P. aeruginosa RNA
Choice Index to E. coli
1.0
0.5
0.0
-0.5
-1.0
ns
*
ns
WT
ASI(-)
E
P. aeruginosa Exposure
RNA
Intestine-wide Distention
NPR-1
ASI
AWB AWC
Hyperoxia Avoidance
TAX-2/4
TAX-2/4
TAX-2/4
P. aeruginosa Avoidance
E. faecalis Exposure
Anterior Intestinal Distention
NPR-1
AWB AWC ASE
Hyperoxia Avoidance
TAX-2/4
TAX-2/4
E. faecalis Avoidance

Figure 5

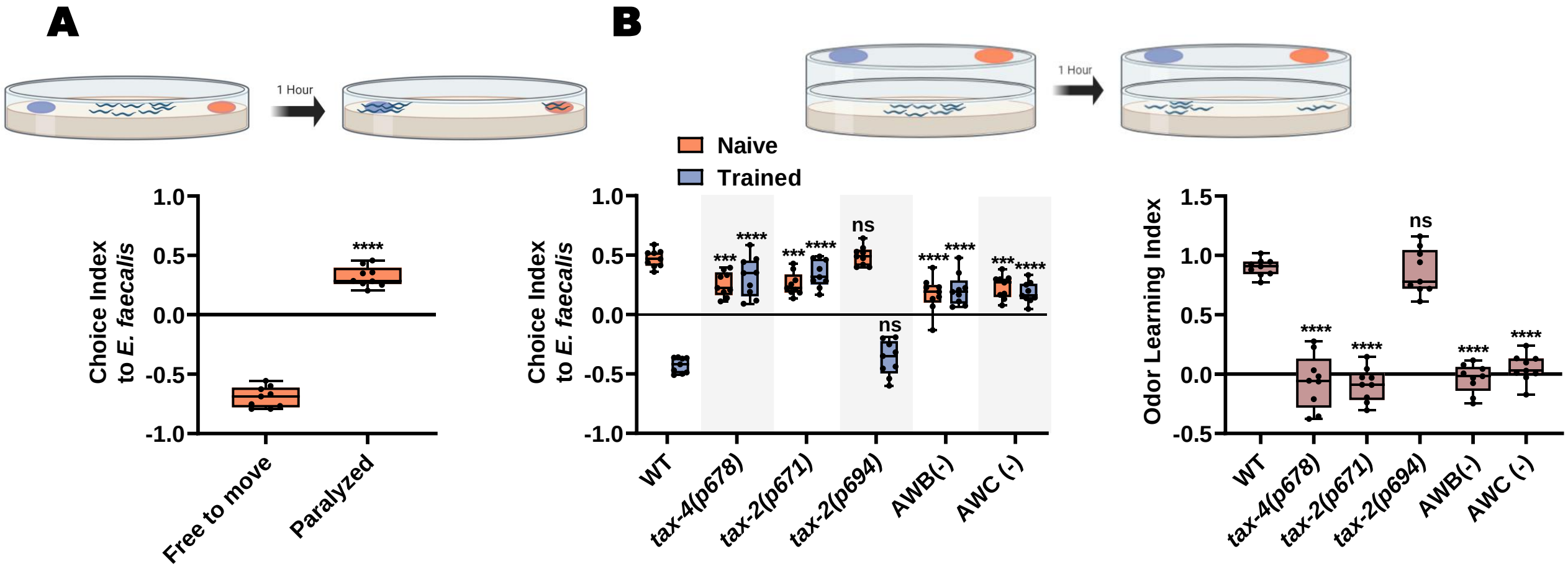
A
1 Hour
Choice Index to E. faecalis
1.0
0.5
0.0
-0.5
-1.0
****
Free to move
Paralyzed
B
1 Hour
Naive
Trained
Choice Index to E. faecalis
1.0
0.5
0.0
-0.5
-1.0
***
****
***
****
ns
ns
****
****
***
****
WT
tax-4(p678)
tax-2(p671)
tax-2(p694)
AWB(-)
AWC (-)
Odor Learning Index
1.5
1.0
0.5
0.0
-0.5
ns
****
****
****
****
WT
tax-4(p678)
tax-2(p671)
tax-2(p694)
AWB(-)
AWC (-)

Figure 6

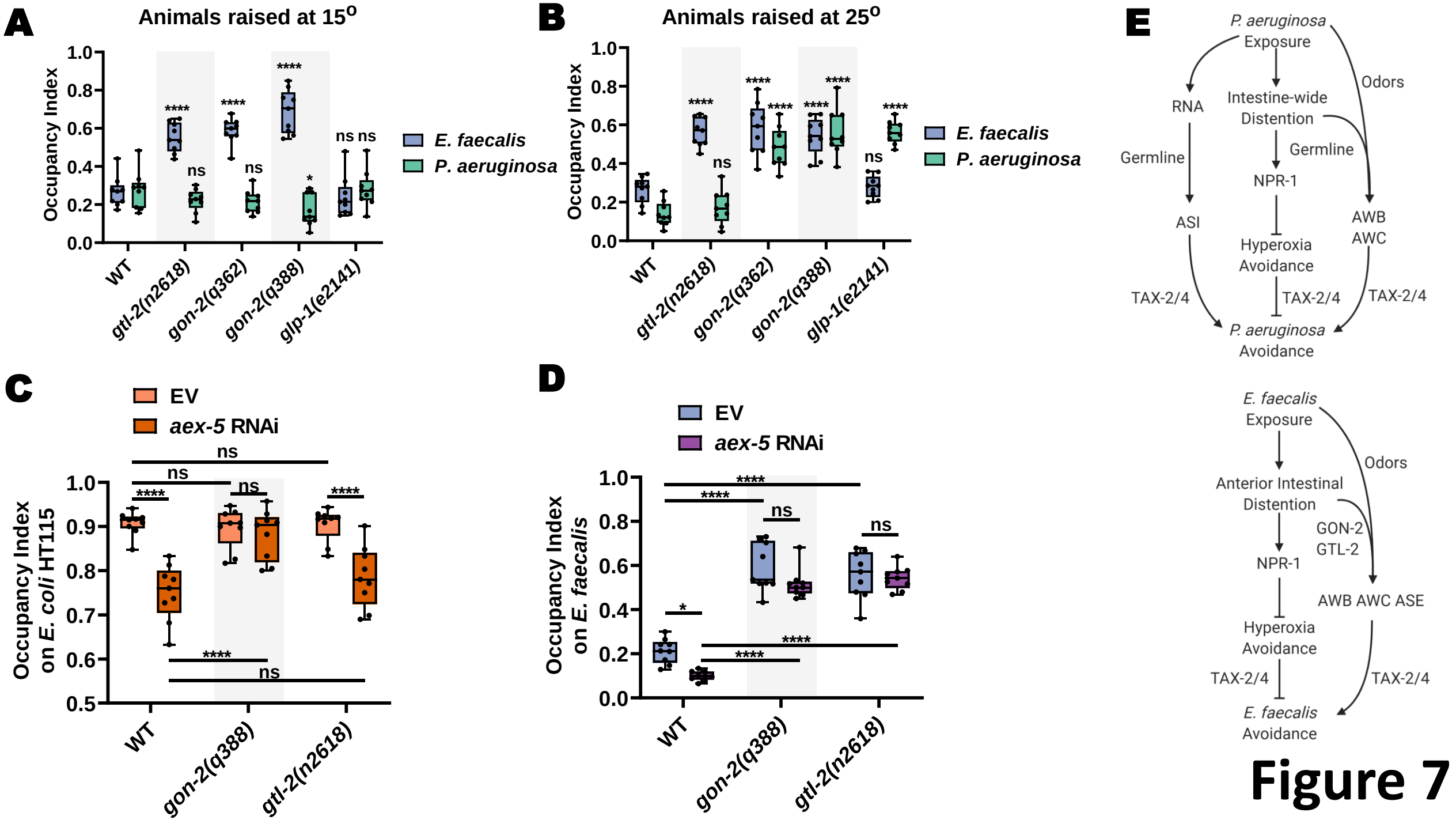
A
Animals raised at 15°
Occupancy Index
1.0
0.8
0.6
0.4
0.2
0.0
****
ns
****
ns
****
*
ns ns
WT
gtl-2(n2618)
gon-2(q362)
gon-2(q388)
glp-1(e2141)
E. faecalis
P. aeruginosa
B
Animals raised at 25°
Occupancy Index
1.0
0.8
0.6
0.4
0.2
0.0
****
ns
****
****
****
****
ns
****
WT
gtl-2(n2618)
gon-2(q362)
gon-2(q388)
glp-1(e2141)
E. faecalis
P. aeruginosa
E
P. aeruginosa
Exposure
Odors
RNA
Intestine-wide
Distention
Germline
Germline
NPR-1
ASI
AWB
AWC
Hyperoxia
Avoidance
TAX-2/4
TAX-2/4
TAX-2/4
P. aeruginosa
Avoidance
C
EV
aex-5 RNAi
ns
ns
****
ns
****
Occupancy Index
on E. coli HT115
1.0
0.9
0.8
0.7
0.6
0.5
****
ns
WT
gon-2(q388)
gtl-2(n2618)
D
EV
aex-5 RNAi
****
****
ns
ns
*
****
****
Occupancy Index
on E. faecalis
1.0
0.8
0.6
0.4
0.2
0.0
WT
gon-2(q388)
gtl-2(n2618)
E. faecalis
Exposure
Odors
Anterior Intestinal
Distention
GON-2
GTL-2
NPR-1
AWB AWC ASE
Hyperoxia
Avoidance
TAX-2/4
TAX-2/4
E. faecalis
Avoidance

Figure 7

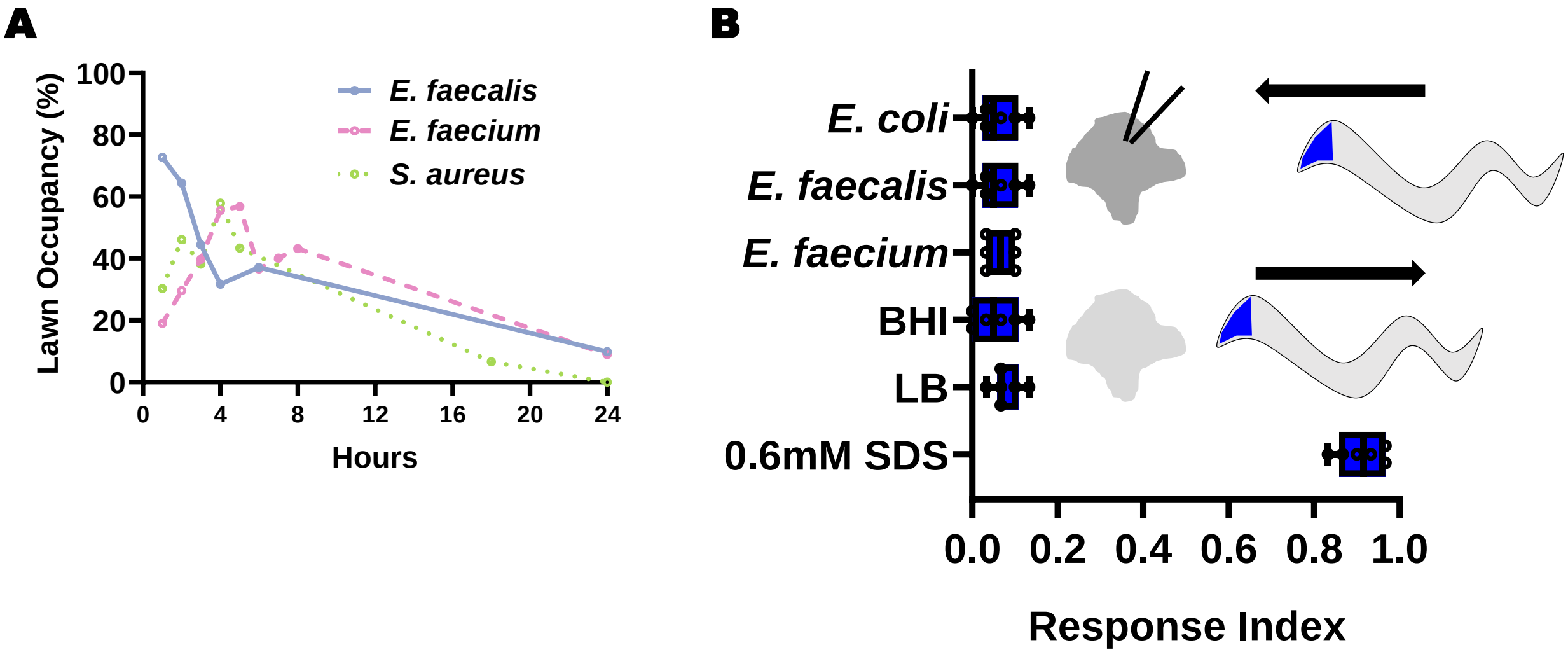

Figure 1 – Supplement 1

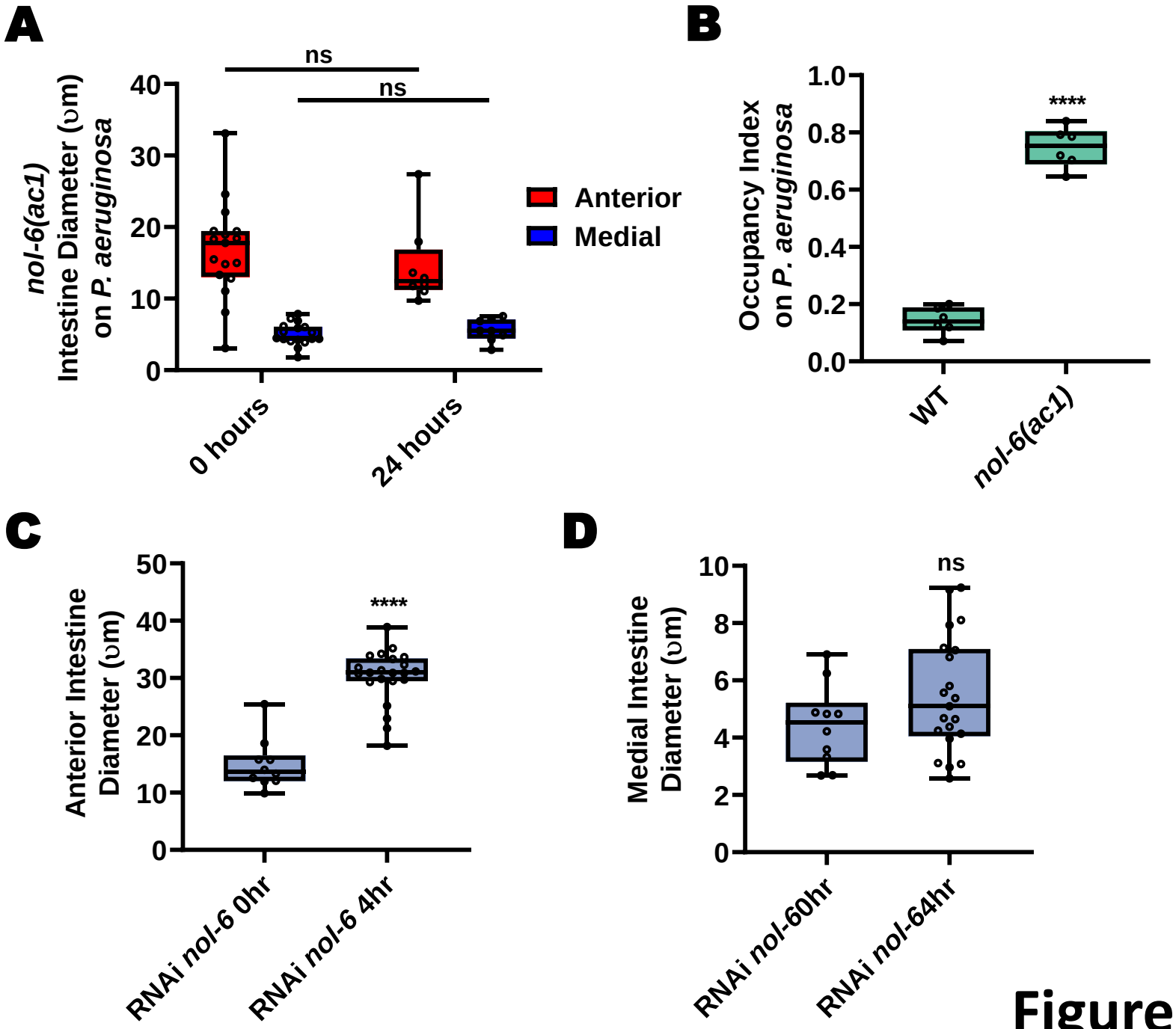

Figure 2 – Supplement 1

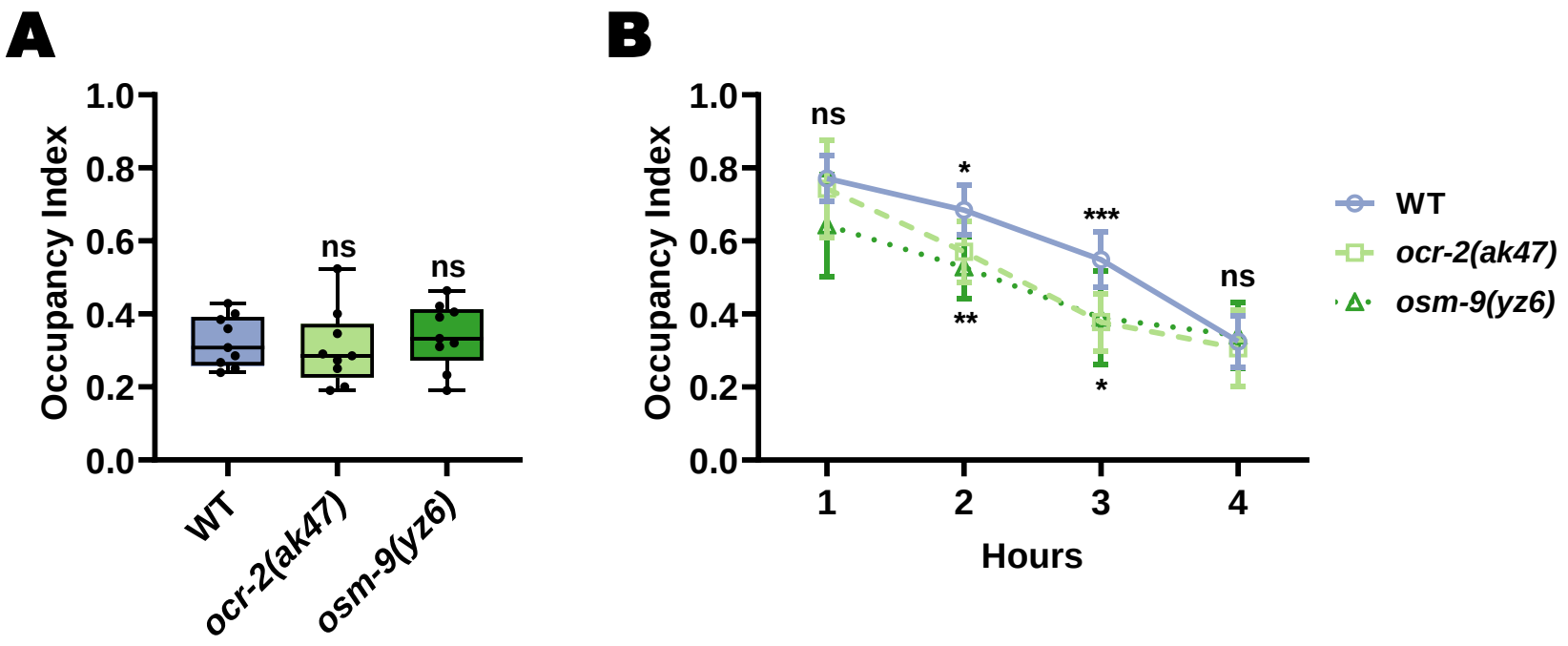

Figure 4 – Supplement 1

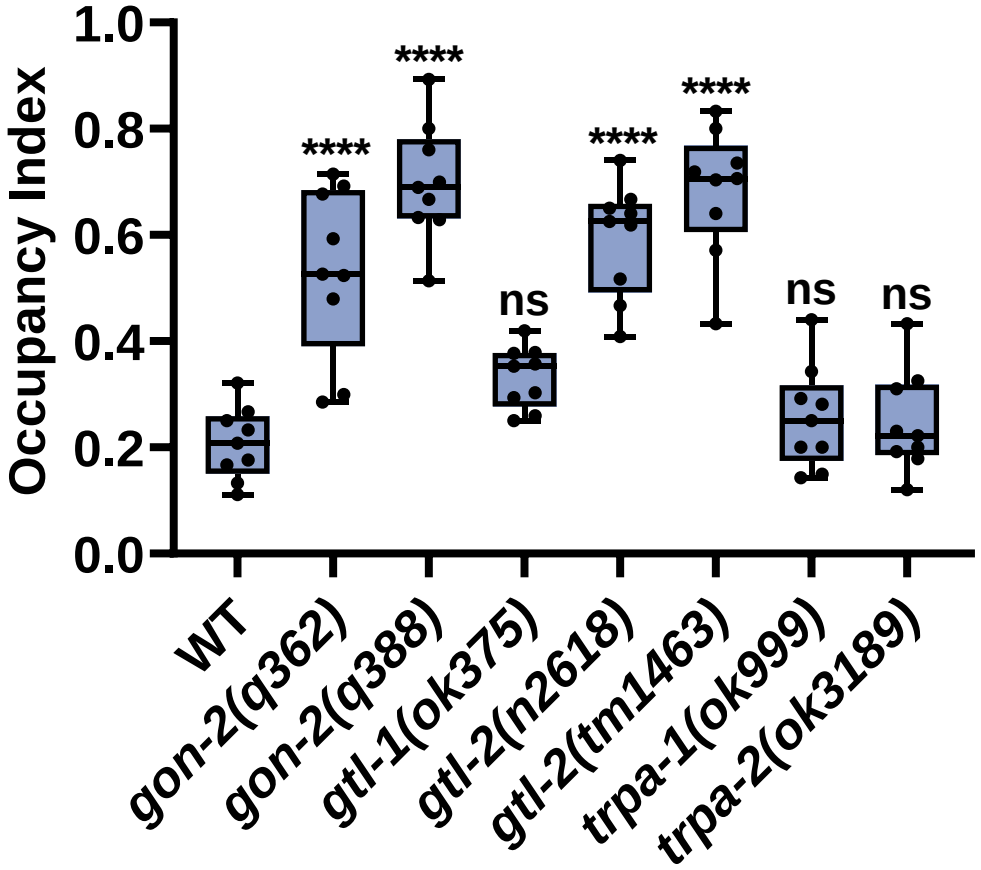

Figure 7 – Supplement 1

bioRxiv preprint doi: https://doi.org/10.1101/2020.12.18.423492; this version posted December 19, 2020. The copyright holder for this preprint (which was not certified by peer review) is the author/funder, who has granted bioRxiv a license to display the preprint in perpetuity. It is made available under aCC-BY-NC-ND 4.0 International license.

Reagent type (species) or resource	Designation	Source or reference	Identifiers	Additional information
Strain, strain background (*Escherichia coli*)	OP50	*Caenorhabditis* Genetics Center	OP50	
Strain, strain background (*E. coli*)	OP50-GFP	*Caenorhabditis* Genetics Center	OP50-GFP	
Strain, strain background (*E. coli*)	HT115	Source BioScience	HT115	
Strain, strain background (*Pseudomonas aeruginosa*)	PA14	Frederick M. Ausubel laboratory	PA14	
Strain, strain background (*P. aeruginosa*)	PA14-GFP	Frederick M. Ausubel laboratory	PA14-GFP	
Strain, strain background (*Enterococcus faecalis*)	OG1RF	Danielle A. Garsin laboratory	OG1RF	
Strain, strain background (*E. faecalis*)	OG1RF-GFP	Danielle A. Garsin laboratory	OG1RF-GFP	
Strain, strain background (*E. faecalis*)	OG1RF ΔfsrB	Danielle A. Garsin laboratory	OG1RF ΔfsrB	
Strain, strain background (*E. faecium*)	E007	Danielle A. Garsin laboratory	E007	
Strain, strain background (*Staphylococcus aureus*)	NCTC8325	National Collection of Type Cultures	NCTC8325	
Strain, strain background (*Caenorhabditis elegans*)	N2 Bristol	*Caenorhabditis* Genetics Center	N2	
Strain, strain background (*C. elegans*)	*npr-1(ad609)*	*Caenorhabditis* Genetics Center	CX4544	
Strain, strain background (*C. elegans*)	*npr-1(ok1447)*	*Caenorhabditis* Genetics Center	CX10	
Strain, strain background (*C. elegans*)	*ocr-2(ok47)*	*Caenorhabditis* Genetics Center	PR671	
Strain, strain background (*C. elegans*)	*osm-9(ky10)*	*Caenorhabditis* Genetics Center	PR694	
Strain, strain background (*C. elegans*)	*gcy-35(ok769); npr-1(ad609)*	Aballay laboratory		
Strain, strain background (*C. elegans*)	*tax-2(p694); npr-1(ad609)*	Aballay laboratory		
Strain, strain background (*C. elegans*)	*tax-4(p678); npr-1(ad609)*	Aballay laboratory		
Strain, strain background (*C. elegans*)	*tax-2(p671)*	*Caenorhabditis* Genetics Center	PR678	
Strain, strain background (*C. elegans*)	*tax-2(p694)*	*Caenorhabditis* Genetics Center	DA609	
Strain, strain background (*C. elegans*)	*tax-4(p678)*	*Caenorhabditis* Genetics Center	RB1330	
Strain, strain background (*C. elegans*)	*tax-2(p694); lin-15&lin-15A(n765); dbEx723[gcy-32p::tax-2(cDNA)::SL2::GFP + lin-15(+)*	*Caenorhabditis* Genetics Center	AX2159	
Strain, strain background (*C. elegans*)	*tax-2(p694); lin-15&lin-15A(n765); dbEx724[flp-6p::tax-2(cDNA)::SL2::GFP + lin-15(+)*	*Caenorhabditis* Genetics Center	AX2161	
Strain, strain background (*C. elegans*)	*che-1(p680)*	*Caenorhabditis* Genetics Center	PR680	ASE(-)
Strain, strain background (*C. elegans*)	*pelsi1713 [sra-6p::mCasp-1 + unc-122p::mCherry]*	*Caenorhabditis* Genetics Center	JN1713	ASH(-)
Strain, strain background (*C. elegans*)	*oyIs84 [gpa-4p::TU#813 + gcy-27p::TU#814 + gcy-27p::GFP + unc-122p::DsRed]*	*Caenorhabditis* Genetics Center	PY7505	ASI(-)
Strain, strain background (*C. elegans*)	*pelsi1715 [str-1p::mCasp-1 + unc-122p::GFP]*	*Caenorhabditis* Genetics Center	JN1715	AWB(-)
Strain, strain background (*C. elegans*)	*oyIs85 [ceh-36p::TU#813 + ceh-36p::TU#814 + srtx-1p::GFP + unc-122p::DsRed]*	*Caenorhabditis* Genetics Center	PY7502	AWC(-)
Strain, strain background (*C. elegans*)	*agIs26 [clec-60p::GFP + myo-2p::mCherry]*	*Caenorhabditis* Genetics Center	JIN810	
Strain, strain background (*C. elegans*)	*unc-119(ed3); eEx650 [ilys-3p::GFP + unc-119(+)]*	*Caenorhabditis* Genetics Center	CB6710	
Strain, strain background (*C. elegans*)	*nol-6(ac1)*	*Caenorhabditis* Genetics Center	AY1	
Strain, strain background (*C. elegans*)	*eat-5(ad1402)*	*Caenorhabditis* Genetics Center	DA1402	
Strain, strain background (*C. elegans*)	*gtl-2(n2618)*	*Caenorhabditis* Genetics Center	CZ9957	
Strain, strain background (*C. elegans*)	*gon-2(q362)*	*Caenorhabditis* Genetics Center	EJ26	
Strain, strain background (*C. elegans*)	*gon-2(q388)*	*Caenorhabditis* Genetics Center	EJ1158	
Strain, strain background (*C. elegans*)	*glp-1(e2141)*	*Caenorhabditis* Genetics Center	CB4037	
Strain, strain background (*C. elegans*)	*gtl-1(ok375)*	*Caenorhabditis* Genetics Center	VC244	
Strain, strain background (*C. elegans*)	*gtl-2(tm463)*	*Caenorhabditis* Genetics Center	LH202	
Strain, strain background (*C. elegans*)	*trpa-1(ok999)*	*Caenorhabditis* Genetics Center	RB1052	
Strain, strain background (*C. elegans*)	*trpa-2(ok3189)*	*Caenorhabditis* Genetics Center	TQ233	
Software, algorithm	GraphPad Prism 8	GraphPad Software		https://www.graphpad.com/scientific-software/prism/
Software, algorithm	ImageJ	NIH		https://imagej.nih.gov/ij/
Software, algorithm	Leica LAS v4.6	Leica		https://www.leica-microsystems.com/
Other	Hypoxia chamber	STEMCELL Technologies	CAT# 27310	https://www.stemcell.com/products/hypoxia-incubator-chamber.html